Fe-Mo-oxide of spinel structure for methanol oxidation

- Synthesis development and catalytic performance

by

Maria Thulin

Department of Chemical Engineering
Lund University

June 2016

Supervisor: **Assoc. Prof. Christian Hulteberg**
Co-supervisor: **Robert Häggblad, Catalyst R&D Manager JM Formox**
Examiner: **Associate Senior Lecturer Helena Svensson**

Picture on front page: Different stages of catalyst material, photo by Maria Thulin.

Postal address	**Visiting address**	**Telephone**
P.O. Box 124	Getingevägen 60	+46 46-222 82 85
SE-221 00 Lund, Sweden		+46 46-222 00 00
Web address		**Telefax**
www.chemeng.lth.se		+46 46-222 45 26

Preface

During the last months, several persons have been involved and helped me to perform and complete this degree project. I would like to send my gratitude to my supervisor Robert Häggblad who has bared with all my questions and have had several helpful inputs.

I would also like to thank the R&D group in Perstorp for making me feel welcome and for all help regarding equipment: Kim Wong, Peter Haack, Kaisa Kisko, Peter Harrysson, Johan Holmberg, Lars Schüler and Sarah Axelsson.

Abstract

The aim of this master thesis was to investigate a Fe-Mo-oxide catalyst of spinel structure for methanol oxidation to produce formaldehyde and determine if the spinel could be an alternative to the commercial Formox catalyst used today. This included firstly, synthesising the catalyst to get more knowledge of the formation of the structure and secondly, determine the activity, selectivity to formaldehyde and stability of the catalyst. A literature review was performed and several synthesis methods to form a Fe/Mo spinel were found. The method that was most commonly used in previous work was precipitation in combination with H_2-reduction and thus it was selected to use for synthesis in this project. Spray drying in combination with H_2-reduction was also chosen to move forward with. The experimental part of the project focused on: synthesis of spinel catalyst, catalyst characterisation and activity and stability measurements. The catalyst synthesis included formation of precursors (precipitation or spray drying), which was prepared and performed before this project, and reduction by hydrogen. For the reduction experiments, some parameters were chosen to vary to learn more about at what conditions the spinel phase is favoured. All synthesised catalysts were characterised; to obtain the present phases in the catalyst an X-ray diffraction analysis was performed and to measure the specific surfaces a Brunauer-Emmett-Teller-analysis was executed. The results showed that it was more difficult to synthesise pure spinel phase when the Mo-content was high.

After reduction and characterisation some catalysts were selected for activity and stability measurements. These measurements aimed to find the catalytic performance of the spinels and compare it to the commercial catalyst used in the process. The activity and ageing tests (stability measurements) were thus constructed to imitate the Formox process in terms of temperatures and reactor feed. Results from the activity tests showed that the selectivity to formaldehyde is lower than for the present Formox catalyst. The most promising spinel from the activity measurements was then used for stability measurements and this test showed better results; the formaldehyde selectivity increased over time. An inductively coupled plasma analysis was performed and it was found that all molybdenum was maintained from the ageing test which is a promising catalyst quality.

Sammanfattning

I detta examensarbete har det övergripande målet varit att undersöka en Fe-Mo-oxid av spinell struktur och att använda den som katalysator vid metanoloxidation för att producera formaldehyd. Detta har gjorts för att utreda huruvida en sådan katalysator står sig mot den kommersiella Formox-katalysatorn som används idag. Arbetet inkluderade att syntetisera och öka förståelsen vid bildandet av spinell-strukturen och att bestämma katalytiska egenskaper såsom aktivitet, formaldehydselektivitet och stabilitet. En litteraturstudie gjordes för att finna lämpliga metoder för att framställa spinellen. En metod som har använts mycket i tidigare arbete var utfällning i kombination med H_2-reduktion och därför var denna metod vald att gå vidare med i den experimentella delen. Spraytorkning i kombination med H_2-reduktion valdes också ut för att användas. Den experimentella delen avgränsades till: katalysatorsyntes, katalysator karaktärisering och aktivitets- och stabilitetsmätningar. Syntesdelen inkluderade bildandet av Fe-Mo-oxiden (utfällning eller spraytorkning) och även H_2-reduktion av denna för bildandet av själva spinell-strukturen. Utfällning och spraytorkning förbereddes och utfördes innan detta examensarbetes början. För reduktionsexperimenten valdes några parametrar ut att varieras för att undersöka under vilka betingelser spinell-strukturen bildas. De bildade katalysatorerna karaktäriserades med röntgendiffraktion och yt-analys och resultaten från analyserna visade att det var svårare att framställa ren spinell-fas vid högre molybdenhalter i katalysatorn.

Efter reduktion och karaktärisering valdes några lovande katalysatorer ut för aktivitets-och stabilitetsmätningar. Dessa utformades till att efterlikna Formox-processen i avseende på temperatur och reaktantgas eftersom katalysatorerna skulle jämföras med den kommersiella katalysatorn. Resultaten från aktivitetsmätningarna visade på lägre formaldehydselektivitet hos spinellerna än för den nuvarande Formox-katalysatorn. Den mest lovade katalysatorn från aktivitetstesterna användes därefter för åldringstest (stabilitetsmätning) och detta visade på bättre resultat; formaldehydselektiviteten ökade med tiden. En induktivt kopplad plasma-analys visade även att all molybden bibehölls under stabilitetsmätningen vilket är en lovande egenskap.

Contents

1 Introduction

Ever since the Formox process was developed 1959, the operating catalyst has been an iron molybdenum oxide. Physical properties of the process have changed, enabling higher productivity in a more efficient way, but the chemical composition of the catalyst has remained unaltered. An interesting path to increase productivity even more is hence to look into a new chemical composition and structure of the catalyst. An iron molybdenum oxide of spinel structure is a possible alternative which has shown interesting properties when it comes to stability and catalyst ageing. However, the selectivity and activity of the spinel structure catalyst still needs further research to match the present Formox catalyst. In this degree project the Fe-Mo-oxide of spinel structure was investigated to gain more knowledge and examine its future possibilities as a methanol oxidation catalyst.

1.1 Aim

The aim of this master thesis project was to investigate an iron molybdenum catalyst with a spinel structure. Two sub-goals were set up; the first sub-goal was to synthesise the spinel by reduction with hydrogen varying the reaction conditions and by doing so obtaining a better knowledge of at which conditions the spinel phase will be favoured. The second sub-goal mattered determination of activity, selectivity toward formaldehyde and stability of the synthesised catalysts. This sub-goal was set up to examine the catalytic performance and hence determine if this catalyst is an alternative to the commercial catalyst.

1.2 Disposition

This report begins with a literature review that presents a background to formaldehyde production, the Formox process, including a description of the commercial catalyst today, and catalysts of spinel structure. This is followed by an experimental part where the three main parts are: catalyst synthesis, catalyst characterisation and catalyst performance. Denominations that are used in this report are presented in this section as well, see 3.1. Relevant and important results are then presented in Results and these results are evaluated in Discussion. Conclusions of the experimental results and suggestions of future work are then presented in section 6 and 7. Appendices finalise the report and in this section more details about the performed experiments and corresponding results can be found.

2 Literature review

2.1 Formaldehyde

Methanal, commonly known as formaldehyde, is the simplest aldehyde and has the chemical formula CH_2O. It has become one of the world's most important chemicals and in 2015 the demand for formaldehyde was 45 Mt/yr [1]. It is mainly used as a precursor for production of other materials and chemicals. The wide range of applications include industries that manufacture plastics, lubricating oils and surface coatings, but the largest amount of formaldehyde is used for production of resins (condensates of formaldehyde combined with chemicals such as urea). The resins are then primarily used for production of adhesives, impregnating and molding materials, utilised in the wood and textile industry [2, 3, 4].

At ambient temperature, formaldehyde is a colourless gas that is irritating for eyes and skin. Hence, when handling this chemical, it is often dissolved into water which then has the commercial name formalin. By adding an inhibitor or stabiliser to the formalin, oxidation and polymerisation will be supressed. A commonly used inhibitor is methanol and chemicals such as methyl- and ethylcelluloses and poly(vinyl alcohol)s are utilised as stabilisers [4]. Some physical and chemical properties are displayed in Table 2.1.

Table 2.1. Physical and chemical properties of formaldehyde.

Property	Value	Ref.
Lower/Upper explosion limit	7/73 mol%	[5]
Ignition temperature	430 °C	[5]
Boiling point (at 1 atm pressure)	-19 °C	[6]
Melting point (at 1 atm pressure)	-118 °C	[6]
Molar mass	30.016 g/mol	

2.2 Production of formaldehyde

In 1859, Alexander Mikhailovich Butlerov was first to synthesise formaldehyde by hydrolysing methylene acetate. Eight years later, August Wilhelm von Hoffman succeeded in producing formaldehyde by reacting methanol with air over a platinum spiral catalyst, establishing the foundation of processes used today. Industrial production and development of this process continued from circa 1900 and silver catalysts were patented. Today, several processes still utilize catalysts based on silver, known as silver processes [2, 3]. These silver processes are one out of two dominating pathways for formaldehyde production; the other pathway is through a process commonly called the oxide process.

2.2.1 The oxide process

Several different kinds of selective oxide processes have been patented since 1921. Generally, this process is carried out in a reactor with a metal oxide catalyst, often an iron molybdenum oxide. Reaction temperatures vary between 250 to 400°C and since the reaction is exothermic, external cooling is required to stabilise the process. A methanol- excess air mixture is used as reactant and the methanol content varies between 6-11 vol% [7] which is below the lower

explosion limit for methanol. Higher methanol concentrations can be used if several physical improvements on process and catalyst have been made, but these concentrations are still much lower than in the silver process [2, 8, 9].

2.2.2 The silver process

The main reactions when using a silver catalyst are shown below in reaction 2.1-2.3. While formaldehyde is formed only by methanol oxidation in the oxide process, formaldehyde is produced by partial methanol oxidation (reac. 2.2) but also through dehydrogenation (reac. 2.1) in the silver process. Normal operating temperature is high; 600-720°C but the exact temperature depends on the methanol content in the air-methanol mixture that is inserted into the system for reaction. The methanol concentration is often around 50 vol%, which is, unlike the oxide process, well above the upper explosion limit for methanol. The silver process is generally easier to operate but more costly and the silver catalyst is generally more sensitive to iron-group impurities than a molybdenum-iron oxide catalyst [2, 8, 9].

$$CH_3OH \leftrightarrow CH_2O + H_2 \qquad \text{(reac. 2.1)}$$

$$CH_3OH + 1/2O_2 \rightarrow CH_2O + H_2O \qquad \text{(reac. 2.2)}$$

$$H_2 + 1/2O_2 \rightarrow H_2O \qquad \text{(reac. 2.3)}$$

2.3 The Formox process

The Formox process is based on the oxide process and uses iron molybdenum oxide as catalyst (section 2.4.1). As can be seen in Figure 2.1, the main components in the process are a condenser, reactor, vaporizer and absorber. The emission control system (ECS unit) and steam generator are upgrades and recover energy from the process, but in the ECS unit any organic component in the off gas is oxidised to CO_2 and water over a metal catalyst [10]. As can be seen in Table 2.2, the selectivity toward formaldehyde is 92-95 %. The rest of the methanol will form by-products and the by-products with most significance are: dimethylether (DME), methylformiate (MF), dimethoxymethane (DMM), CO and CO_2 [9]. Along with the formaldehyde selectivity, Table 2.2 shows typical numbers from the Formox process.

Table 2.2. Specifications from the Formox process.

Variable	Typical number	Reference
Methanol concentration in feed	6-11 vol%	[7]
Conversion	95-99 %	[2]
Overall plant yield	90-94 %	[7]
Selectivity to formaldehyde	92-95 %	[7]
Final product concentrations	Formaldehyde: 37-57 wt% Methanol: 0.3-0.5 wt% (in 37 wt% formaldehyde)	[10]

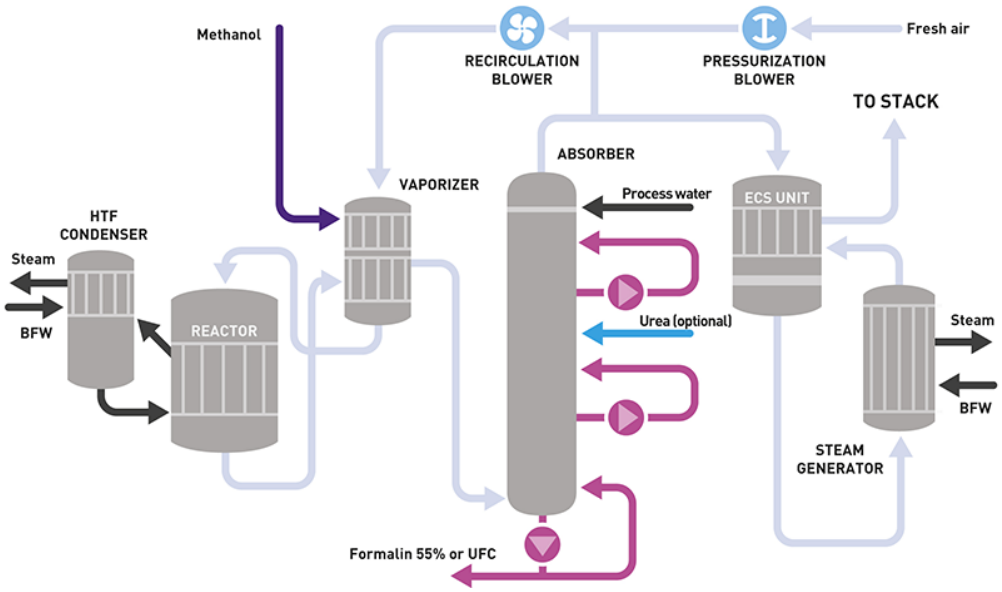

Figure 2.1. Flowsheet of the Formox process, reprinted with permission [10].

2.4 Catalysts for formaldehyde production

Heterogeneous catalysts in industrial scale have been used ever since the 17th century to control kinetics and directions of chemical reactions. Many heterogeneous catalysts consist of a metal and/or a metal oxide, which is also the case for catalysts for selective oxidation reactions (involves formaldehyde production). Section 2.4.1 and 2.4.2 describe the properties of, and reaction kinetics over, the most commonly used catalysts in corresponding formaldehyde production process.

Three important concepts in catalysis that will be considered in the experimental study of this project are selectivity, activity and stability/deactivation of the catalyst bed. The selectivity determines the ratio of product formed from reactant and the concept is normally used to decide the catalyst's capability of generating desired product. The activity normally refers to the rate at which the chemical reaction proceeds towards chemical equilibrium. Selectivity and activity both varies with parameters such as pressure, temperature and chemical composition. Loss of selectivity or activity is called deactivation, which can be caused by several reasons: poisoning, fouling, reduction of active area and loss of active components [11].

2.4.1 Iron molybdenum catalyst

The operating catalyst in the Formox process today consists of two crystalline phases: MoO_3 and $Fe_2(MoO_4)_3$. The chemical composition has basically remained the same over the years and improvements of productivity have mainly occurred due to physical changes of the process [3]. However, research on alternative catalysts has occurred where the iron molybdate has been doped with small amounts of other transition metals such as vanadium [12] or where the Fe/Mo ratio was varied [3].

The oxidation of methanol to formaldehyde over a molybdenum iron catalyst is of redox type mechanism, Figure 2.2. When methanol is oxidised and formaldehyde is synthesised, the catalyst surface is reduced and for the catalyst surface to be re-oxidised, oxygen has to be provided from the surrounding gas or the catalyst bulk. According to Carbucicchio et al. [13], the reduction of the catalyst surface starts at lower temperatures than the re-oxidation. Due to excess temperatures and lack of re-oxidation of the catalyst surface, MoO_3 volatiles from the surface and the active catalyst surface will decrease. Naturally, this reduces the selectivity since Mo is the more selective species, but the mechanical strength and activity of the catalyst will also go down [8, 9, 14]. To reduce this undesirable effect, MoO_3 is added during preparation of the catalyst but over time the molybdenum fraction still will decrease. Also, if the catalyst is subjected to a tougher environment during reaction, such as higher temperature, pressure or methanol inlet concentration, the loss of molybdenum will be greater. Consequently, the lifetime of the catalyst depends on reaction conditions and in literature the reported lifetime varies between 6-12 months [8] and 12-18 months [4].

Two redox reaction mechanisms have been proposed for methanol oxidation over an iron molybdenum catalyst: Langmuir-Hinshelwood and Mars-van Krevelen [9]. Overviews of the mechanisms can be seen in Figure 2.3. Traditionally, Mars-van Kreleven has been used to illustrate the reaction [9, 15, 16] but there are studies that suggest Langmuir-Hinshelwood type dependency at higher methanol concentrations [17]. It should be added that the above mentioned studies operated on different reactors under different conditions. For example, a differential reactor was used in the study that suggested Langmuir-Hinshelwood and since this reactor type operates with low conversion rates, temperature gradients within the catalyst region were avoided [17]. In [16] a continuous flow reactor was used and a larger conversion range was considered; the conversion was varied from 0.2 – 95%.

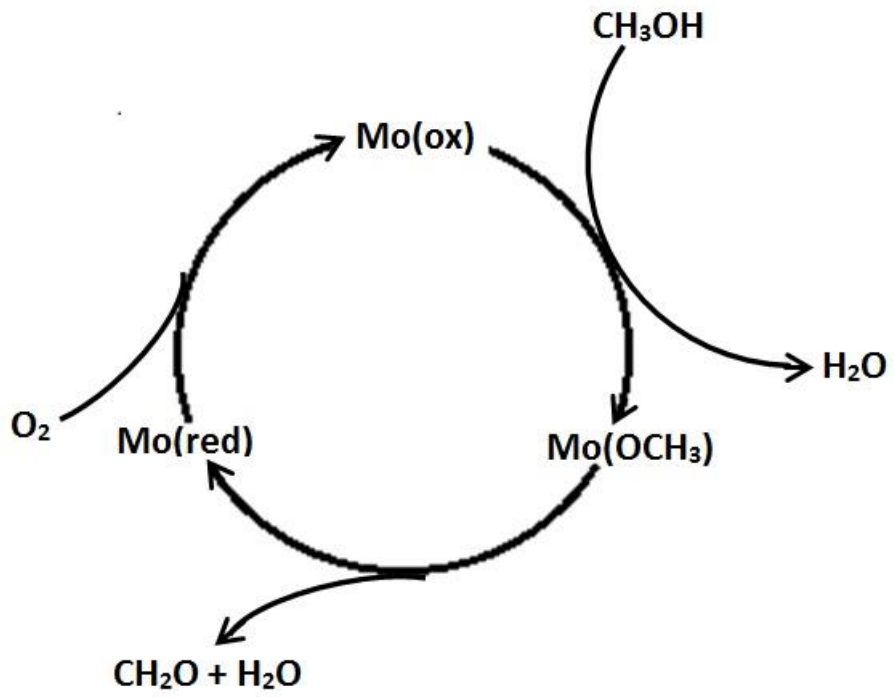

Figure 2.2. The redox mechanism of methanol oxidation over a molybdenum iron oxide.

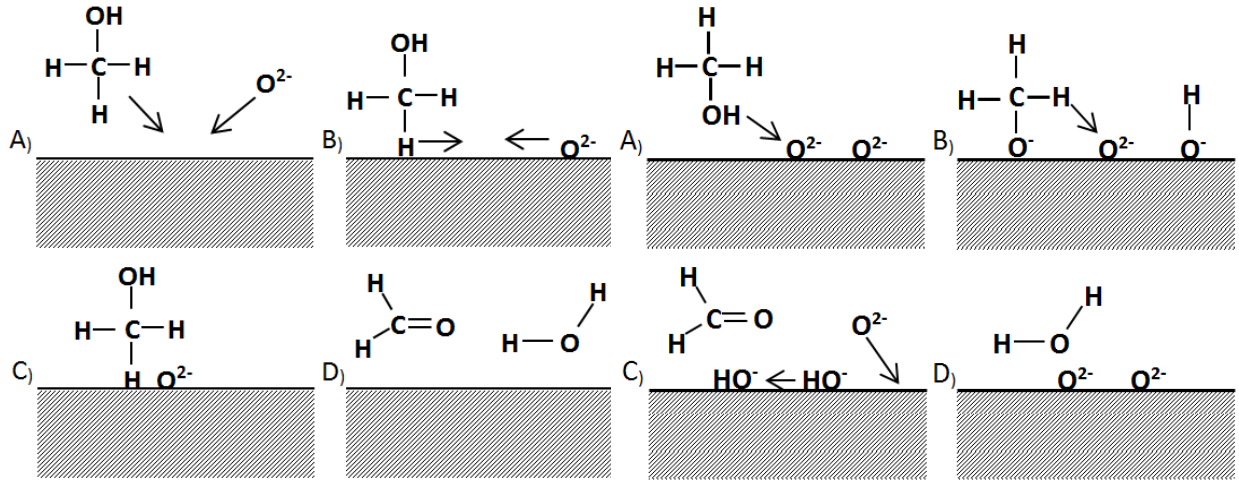

Figure 2.3. Left: Langmuir-Hinselwood mechanism for methanol oxidation to formaldehyde. Right: Mars-van Krevelen mechanism for methanol oxidation to formaldehyde.

2.4.2 Silver catalyst

The catalyst bed in the silver process normally consists of silver wire gauze or silver crystals. Since metallic silver has low catalytic activity for methanol decomposition, it is pre-treated with oxygen. Silver is exposed to oxygen and the oxygen is chemisorbed onto the surface which activates the catalyst. The methanol can then be adsorbed to the surface but the reaction mechanism of methanol to formaldehyde conversion is somewhat unclear [2, 8]. In some studies [18, 19] it is proposed that different atomic oxygen species are present in the reaction sequence and each species has a specific catalytic function. Consequently, it is still hard to decide how much each of the two reaction pathways (reac. 2.1 and reac. 2.2 respectively in section 2.2.2) contributes to the total conversion.

Catalyst lifetime varies, as for iron molybdenum oxide, with process conditions from a couple of months to 2 years [8]. However, the catalyst lifetime also depends on how pure the feed is since the silver catalyst is very sensitive to impurities, such as transition metals and sulphur.

2.5 Catalyst of spinel structure

Spinel is originally the name of the mixed metal oxide $MgAl_2O_4$. The structure of the oxide is classified as a ccp structure of O^{2-} anions where half of the octahedral and 1/8 of the tetrahedral interstices are occupied by Al^{3+} and Mg^{2+} ions respectively. The spinel structure can be written as the general chemical formula: AB_2O_4 [20]. In this report the concept spinel or spinel type will be used for metal oxides with spinel type structure, in other words, not only for the magnesium alumina oxide explained above.

When forming a spinel structure, a redox reaction changing the oxidation state of a metal oxide takes place. The oxidation state of the metal atoms will be modified when the chemical composition is changed, allowing the metal oxide to form a spinel structure. The cations (the metal atoms) in the spinel will then be oxidised when it is exposed to oxygen and to balance

the stoichiometry and maintain the structure, cation vacancies will form. These vacancies allow the crystals to be more flexible; atoms can diffuse through the lattice without altering the spinel structure [21, 22, 23]. The general chemical formula after oxidising the metal oxide can be written as: $AB_2O_{4+\delta}$ [24]. The chemical formula for an iron molybdenum spinel that has been oxidised is $Fe_{3-x-y}Mo_x\square_yO_{4+\delta}$. The iron molybdenum spinel after reduction is black and magnetic but after oxidation the spinels are slightly redder [25].

The possible advantage of using a molybdenum iron spinel over another metal spinel is that molybdenum can exist in oxidation state +6 [26]. This could lead to formation of more vacancies compared to metals with lower oxidation states. Compared to the catalyst in the Formox process used today, a molybdenum iron spinel could probably operate for a longer time. This is due to the flexibility of the spinel structure which could slow down the loss of active species, and in other words, slow down the ageing of the catalyst. Also, it could be possible to operate the spinel under higher pressure and temperature due to its advantageous stable structure. However, catalyst activity measurements that have been performed showed that the spinel areal activity (in mol/(m^2 s)) is slightly lower than activity for the commercial Formox catalyst [22, 23, 24].

2.5.1 Synthesis methods

Spinels containing different metals can be synthesised by several different methods and four of those are presented below in this section. Since this master thesis concerns iron molybdate spinels, this section is focused on how to synthesise only this specific spinel.

2.5.1.1 Precipitation and reduction

Precipitation of iron and molybdenum is the first step of this method to synthesise an iron molybdate spinel. A salt containing iron together with a molybdenum salt is dissolved into water at acidic conditions. Precipitate of iron- and molybdenum hydroxides will form in the solution when pH is increased by adding an alkaline medium [23]. To get a similar precipitation rate of molybdenum and iron, a low initial pH is favourable, followed by a rapid increase to a pH where iron and molybdenum have a similar precipitation rate [25]. To support ageing (particle coarsening), the solution is kept at 50-60°C under continuously stirring for a couple of hours. The precipitated precursor particles are then separated by filtration or centrifugation, washed with water and acetone, and finally dried. In previous research temperatures between 90-110°C have been set points for the drying process [3, 24, 27]. Salts commonly used are $FeNO_3$ and ammonium heptamolybdate [3, 23, 27]. Precipitation can also be performed by titration at a low pH as described in [3]. However, this will not ensure similar precipitation rates of molybdenum and iron [25].

Reduction of the synthesised precursor particles is the second step and takes place under reducing conditions at temperatures between 450-800°C [26]. The reducing agent is often H_2 but CO can also be used. H_2O or CO_2 is also inserted to the system making sure that the iron molybdenum oxide does not over-reduce. Over-reduction will cause the oxide to form other phases than the spinel. An inert gas is normally also used, such as nitrogen or argon. The H_2/H_2O system has been used in several reports with successful results [21, 26, 28]. In some reports, the synthesised spinels were then oxidised in a controlled environment at different

temperatures [21, 26]. Reactions 2.4-2.6 [29] below show main reduction and oxidation equilibrium reactions when iron oxide is reduced by hydrogen (the spinel structure is represented by Fe_3O_4). Figure 2.4 shows a phase diagram for iron oxides at certain temperatures and certain H_2/H_2O ratios. Certainly, the diagram and reactions are not valid for iron molybdenum oxide but it still offers a hint of what temperatures and H_2/H_2O ratios that are needed to form iron molybdate spinels.

$$3Fe_2O_3 + H_2 \leftrightarrow 2Fe_3O_4 + H_2O \quad \text{(reac.2.4)}$$

$$Fe_3O_4 + H_2 \leftrightarrow 3FeO + H_2O \quad \text{(reac.2.5)}$$

$$FeO + H_2 \leftrightarrow Fe + H_2O \quad \text{(reac.2.6)}$$

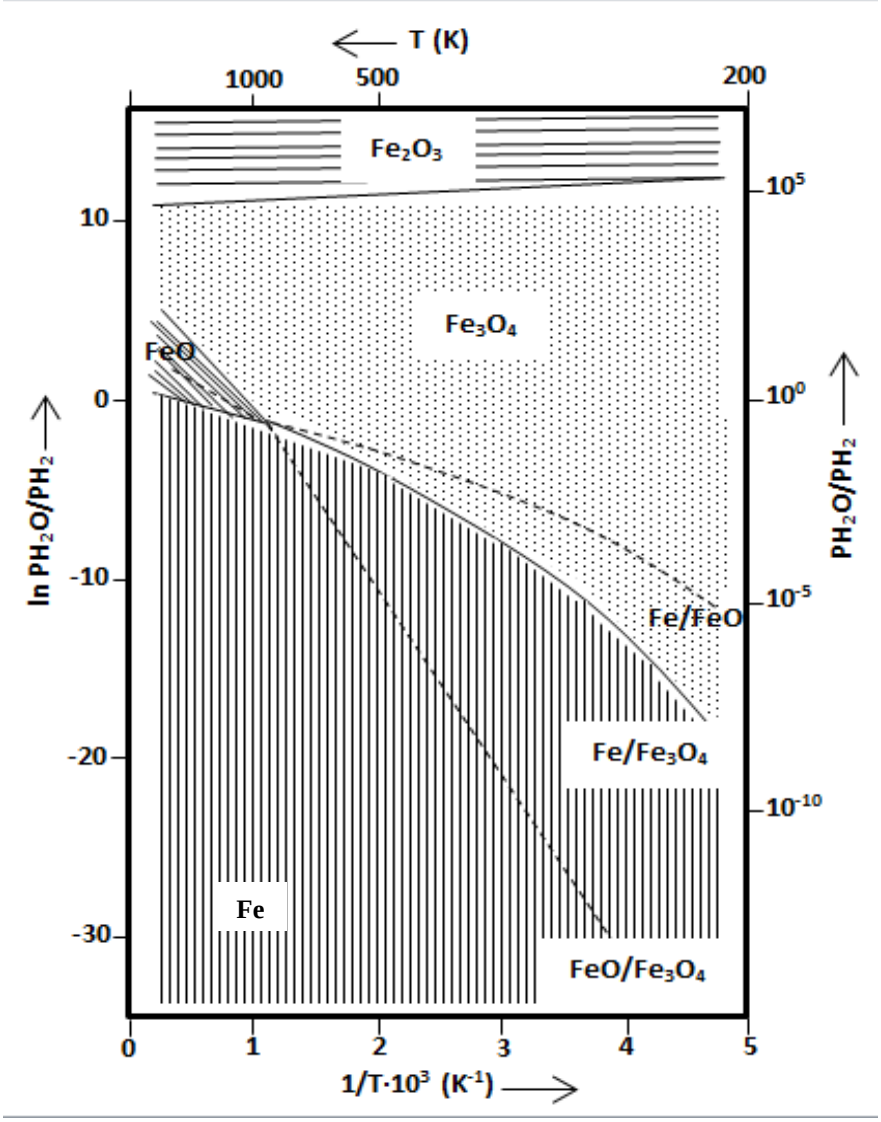

Figure 2.4. Phase diagram for iron oxides at different H_2/H_2O ratios and different temperatures.

2.5.1.2 Spray drying and reduction

Spray drying can be used instead of precipitation to form catalyst precursors. Salt containing molybdenum and iron are dissolved into water and the two solutions are mixed under rigorous stirring. The homogeneous solution is then sprayed into an oven and metal oxide crystals will form [25, 30]. To remove excess nitrates that will solidify during drying, calcination of the product can be performed. The precursors are then reduced in the same manner as explained above in section 2.5.1.1.

Experiments that apply the spray drying technique have been made with successful outcomes; in [31] and [32] metal oxides were dried and used via spray drying. In [32] it was also demonstrated that spray drying is a time effective method and results in a purer product.

2.5.1.3 Oxidation of a suspension

A more complicated but still interesting method to produce spinels is oxidation of a suspension. Salts containing iron at oxidation state 2+ and molybdenum are dissolved in water. An alkaline solution is also prepared by dissolving hydroxide into water. Spinels are synthesised when the alkali solution and an oxidising agent are added to the metal solution. A temperature around 70°C should be maintained during synthesis to promote coarser particles. Finally, the particles should be filtered, washed and dried [33, 34].

2.5.1.4 Reduction by decomposition of a complex

An organometallic complex is first synthesised by reacting a metallic salt with a hydroxy acid, such as citric, lactic, oxalic or malic acid. Metal salts are dissolved into water and the hydroxy acid is added to the aqueous metal solution. After formation of complexes, the solution has to be concentrated and that can be done with a rotavapor. To dehydrate the concentrated solution completely, it is dried under vacuum at 80°C, resulting in a metallic, amorphous foam. Initial heating of this metallic precursor decomposes the complex and generates lightweight metal oxides. Upon further heating, the spinel structure can be formed [35]. Attempts to synthesise spinels applying this method have been made, but several other undesirable metal oxide phases were formed as well [24].

2.6 Remarks from literature review

A spinel structure catalyst could be advantageous over the conventional Mo-Fe oxide since loss of molybdenum seems to be prevented with the spinel structure. From literature it appears as if the spinel is competitive with the commercial catalyst when comparing the selectivity while the activity of the spinel is a bit lower. However, lower activity could contribute to new possibilities when it comes to loading design of the methanol reaction tube, less inert particles could perhaps be used. Reducing the loss of molybdenum contributes to higher stability and it could be possible to run methanol oxidation in a more aggressive environment.

The methods that will be used for experiments in this project are precipitation or spray drying in combination with reduction since they seem to be the least complicated. However, oxidation of suspension is also an interesting synthesis route since no H_2 or CO is required. Precipitation and spray drying for precursor synthesis were executed before the start of this project, and the prepared precursors were then reduced by hydrogen at site Perstorp. According to previous research [24, 26], precipitation or spray drying in combination with reduction seem like promising synthesis routs to produce spinels. The activity and selectivity of the synthesised catalysts should also be investigated and compared to a commercial catalyst to see if the spinels could be an alternative to the commercial catalyst. This can be done by letting methanol oxidise over the catalysts, analysing the outlet gas with a gas chromatograph and calculating the activities and selectivities.

3 Experimental

The experimental part describes methods and techniques that were applied in this thesis project; several methods have been used to synthesise, characterise and obtain the catalytic performance of the catalysts. The majority of the methods have not been explained in detail since it is assumed that the reader has some knowledge of this.

Complete experiment details and calculations for the reduction can be found in appendix B and C while experiment details from catalytic performance can be found in Appendix E and F.

3.1 Experiment and catalyst denomination

The reduction experiments and catalysts were named by denominations which are presented in Table 3.1 below. Denominations of the synthesised catalysts that were tested for catalytic performance are the same as for the experiment names for reduction of precursors. The reference catalyst that is used in the report is the commercial Formox catalyst, KH44L, which is an iron-molybdenum oxide, section 2.4.1.

Table 3.1. Reduction experiment and catalyst denominations used in this report.

Denomination	Parameter
Synthesis method	
SD	Spray Drying
P	Precipitation
Composition	
C1	$Fe_{2.7}Mo_{0.3}$
C2	$Fe_{2.4}Mo_{0.6}$
C3	$Fe_{2.0}Mo_{1.0}$
Water content red. gas	
G1	0.030
G2	0.22
G3	0.61
G4	0.40
Temperatures	
T1	10°C/min
T2	5°C/min

3.2 Catalyst synthesis

In this section, experiments related to the catalyst synthesis are presented and explained. The used method for catalyst synthesis was precipitation or spray drying in combination with hydrogen reduction, see section 3.2.1. Different conditions and methods were investigated to understand the behaviour of an iron molybdenum oxide of spinel structure.

3.2.1 Precursor synthesis

The spray dried precursors were prepared as follows:

One solution containing 1M $FeNO_3$ and one solution containing 1M (metal basis) ammoniumparamolybdate were prepared. The two solutions were then mixed under rigorous stirring for 2 minutes. To obtain different compositions, different volumes of the molybdenum solution were used. The mixed solution was spray dried and the produced particles were washed and oven dried at 80°C for 16 h. Finally, to remove volatile compounds such as ammonium, the particles were calcinated for 30 minutes at 240°C.

The precipitated precursors were prepared as follows:

One solution containing 1M $FeNO_3$ and one solution containing 1M (metal basis) ammoniumparamolybdate were prepared. Also, a 3M solution of ammonia and a 1M solution of acetic acid were prepared. The acid solution was heated to 60°C and ammonia was added to achive pH 3. The two metal solutions were then mixed under rigorous stirring for 2 minutes. To obtain different compositions different volumes of the molybdenum solution were used. The acetic acid solution and the metal solutions were mixed and the resulting mixture was kept at 60°C for 2 h to promote particle coarsening. The precipitate was obtained by centrifugation and washing. Lastly, the particles were oven dried at 80°C for 16 h.

3.2.2 Reduction of precursors

A reduction setup consisting of mass flow controllers (MFC), gas preheater, water vaporiser, reduction oven and a mass spectrometer (MS) were constructed, see Figure 3.1. Below in this section the performed experiments on reduction of catalyst precursor are presented. The total flow of the gas mixture in all experiments was roughly 6,000 Nml/min and it was based on maximum possible nitrogen flow.

Since the spray dried material was a very fine powder, it was tableted and crushed to obtain larger particle sizes, making sure that no particles were pushed through the filters in the reaction tubes. To establish that the particles had an acceptable size, a 250-450 μm and a >450 μm sieve were used. The precipitated precursor particles were only sieved since no tableting was required.

To investigate how the spinel formation behaved at different oven temperatures, 2 different heating rates of the oven were investigated, Table 3.2 experiment RR01:T1 and RR01:T2. 4-5g spray dried precursor mass with composition $Fe_{2.4}Mo_{0.6}$ was placed in the reduction tube. The nitrogen flow was started and when all components had reached its correct starting temperatures (chosen from ‘Vaporisation temperature, Appendix B’), the water pump and hydrogen flow was started. The heating rates of the oven that were used are presented below in Table 3.2. Start and end oven temperature was 150 and 480°C respectively and the total time of heating and reduction at end temperature was 16.5 h. The water content of the gas was hold at 22vol% for these experiments.

To investigate the impact of the H_2/H_2O ratio, the water content of the reduction gas was varied to find where the spinel structure is stable, Table 3.2 experiment RR02:G1 and RR02:G3. The experiment was executed in the same manner as for as above but the heating rate was hold at 5°C/min.

Reduction of precursors with different iron molybdenum ratios and different synthesised methods was performed, experiments R01-SD-C1-R01-P-C3 in Table 3.2. The heating rate and water content that were applied were chosen from previous experiments and after reduction, the spinels were oxidised for 30 minutes by choking the hydrogen and water but adding an air flow of 50 Nml/min to the system.

After considering the XRD-analysis of the spinels, three additional reductions were performed, all under inert heating (no H_2 inserted while the system and catalyst was heated) and moreover, without any specific heating rates. The specifications for these experiments can be seen in Table 3.2, experiment R02-SD-C2 – R02-SD-C3:2.

All performed reduction experiments with corresponding names and specifications are presented in Table 3.2.

Table 3.2. Performed reductions and the specifications of each experiment.

Experiment	**Catalyst specifications**	**Red. Temperature/ Heating rate**	**H_2O content in red. gas (vol%)**
RR01:T1	Spray dried $Fe_{2.4}Mo_{0.6}$	480°C/ 10°C/min	22
RR01:T2	Spray dried $Fe_{2.4}Mo_{0.6}$	480 °C/ 5°C/min	22
RR02:G1	Spray dried $Fe_{2.4}Mo_{0.6}$	480 °C/ 5°C/min	3
RR02:G3	Spray dried $Fe_{2.4}Mo_{0.6}$	480 °C/ 5°C/min	40
R01-SD-C1	Spray dried $Fe_{2.7}Mo_{0.3}$	480 °C/ 5°C/min	22
R01-SD-C2	Spray dried $Fe_{2.4}Mo_{0.6}$	480 °C/ 5°C/min	22
R01-SD-C3	Spray dried Fe_2Mo_1	480 °C/ 5°C/min	22
R01-P-C1	Precipitated $Fe_{2.7}Mo_{0.3}$	480 °C/ 5°C/min	22
R01-P-C2	Precipitated $Fe_{2.4}Mo_{0.6}$	480 °C/ 5°C/min	22
R01-P-C3	Precipitated Fe_2Mo_1	480 °C/ 5°C/min	22
R02-SD-C2	Spray dried $Fe_{2.4}Mo_{0.6}$	480 °C/ inert heating	22
R02-SD-C3:1	Spray dried Fe_2Mo_1	530 °C/ inert heating	3
R02-SD-C3:2	Spray dried Fe_2Mo_1	530 °C/ inert heating	22

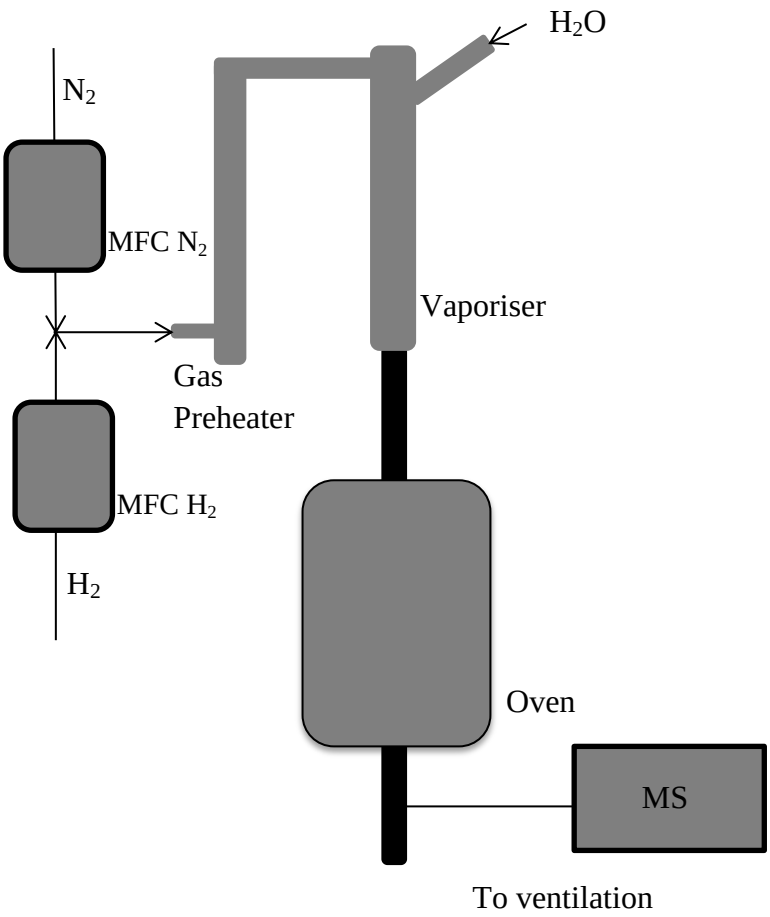

Figure 3.1. Rough draft of reduction setup.

3.3 Catalyst characterisation

Precursors together with fresh and spent spinels were characterised to determine their properties. This section describes which analyses that were performed and what they established.

3.3.1 Present phases (X-ray diffraction, XRD)

XRD-analysis was used to determine which phases that was present in the synthesised catalyst, establishing if the spinel phase was formed. Only fresh catalyst (before methanol oxidation) was sent for XRD-analysis.

3.3.2 Specific surface (BET-analysis)

BET-analysis combined with adsorption of nitrogen measured the specific surface area of the catalysts. All samples were degassed at 250°C for 2 h or more before this analysis was performed. By adsorbing and desorbing nitrogen, the specific area was measured. This analysis was performed on fresh catalyst, i.e. before oxidation of methanol.

3.4 Catalytic performance

To determine the catalyst activity and stability from methanol oxidation to formaldehyde, a methanol oxidation setup including five methanol reactors with heating jacket, preheater, heating tracer after reactors and mass flow controllers was used. The methanol in the feed was oxidised over spinel catalysts and the product gas was analysed with a gas chromatographer from SRI instruments, equipped with a HayeSep C column and HayeSep T column. The gas chromatographer detected the components with a methaniser and flame ionisation detector, FID.

All activity and stability measurements (excluding calibration) had a total flow of 400 Nml/min. The feed going into the reactors was a mixture of methanol, water, oxygen and nitrogen. The methanol and oxygen content were each set to 10vol% of the total flow, the water flow to 3vol% and the nitrogen flow to 77vol% of the total flow. The tube diameter of each reactor was 0.45cm and bed height was roughly 4cm, which resulted in a GHSV of 38000 h^{-1} when the volumetric flow was 400 Nml/min.

3.4.1 Activity measurements

Since the precursor material was sieved before the reduction, the produced spinels mainly had particle sizes between 250-450μm. The spinels were put into the reactors, varying the loading masses together with varying amounts of inert particles, sizes 250-450μm. The activity measurements were performed on R01-SD-C1, R01-P-C1, R02-SD-C3:1 and three different masses of R01-SD-C2. Due to high amounts of other phases in the catalysts, not all of the remaining spinels were tested. The inlet reactor pressure was atmospheric pressure and the total loading mass of all measurements was 1g, which included 0.3g top inert and 0.7g mixture of catalyst together with inert particles. The catalyst mass was varied between 0.1-0.3g to obtain varying conversions.

The activity measurements proceeded for approximately 2.5 h of reaction time for each catalyst and 7.5 h of bypass time. With the obtained peak areas from the gas chromatograph and the calibration curves the concentration of each detected component was calculated in excel. From the concentrations and equation 1, the molar flows could be calculated and by using a carbon balance over the reactions 3.1-3.6, selectivity, activity and conversion of each component were found (using equation 2-4). These calculations were performed in an excel programme. All catalysts used for activity measurements were tested at two temperatures: 300 and 330°C.

3.4.2 Stability and ageing

One of the catalysts that was used for activity measurements was tested for ageing effects, such as Mo-loss over time. The experiment was executed as for activity measurements in terms of reaction conditions but with a reaction interval of approximately 3 days at 300°C. The loading mass was 1g: 0.25g catalyst, 0.45g inert particles in mixture and 0.3g top inert.

The spinel used for stability measurement was analysed by inductively coupled plasma atomic emission spectroscopy (ICP-AES) to determine the iron molybdenum ratio of the sample. This analysis was performed at "Växtekologens lab", Lund University, on fresh and spent catalyst to determine the Mo-escape.

3.5 Calculations

$$CH_3OH + CH_3OH \rightarrow CH_3OCH_3 + H_2O \quad \text{(reac. 3.1)}$$

$$CH_3OH + {}^1/_2\, O_2 \rightarrow CH_2O + H_2O \quad \text{(reac. 3.2)}$$

$$CH_2O + 2CH_3OH \leftrightarrow (CH_3O)_2CH_2 + H_2O \quad \text{(reac. 3.3)}$$

$$CH_2O + {}^1/_2\, O_2 + CH_3OH \rightarrow HCOOCH_3 + H_2O \quad \text{(reac. 3.4)}$$

$$CH_2O + {}^1/_2\, O_2 \rightarrow CO + H_2O \quad \text{(reac. 3.5)}$$

$$CH_2O + O_2 \rightarrow CO_2 + H_2O \quad \text{(reac. 3.6)}$$

$$\dot{n}RT = p\dot{V} \quad \text{(eq. 1)}$$

$$Selectivity_i = \frac{c \cdot \dot{n}_i}{\dot{n}_{MeOH,0} - \dot{n}_{MeOH}} \quad \text{(eq. 2)}$$

$$x = \frac{\dot{n}_{MeOH,0} - \dot{n}_{MeOH}}{\dot{n}_{MeOH,0}} \quad \text{(eq. 3)}$$

$$Activity = \frac{\dot{n}_{MeOH} \cdot x}{m_{cat} \cdot A_{surf,cat}} \quad \text{(eq. 4)}$$

Table 3.3 presents the parameters used for the calculations above.

Table 3.3. Parameters used for calculations in this section.

Denomination	Explanation	Unit
$\dot{n}$	Total molar flow	mol/min
$\dot{V}$	Total gas flow	
$selectivity_i$	Selectivity from methanol toward component i	%
c	Stoichiometric coefficient	-
$\dot{n}_i$	Molar flow of component i out of reactor	mol/min
$\dot{n}_{MeOH,0}$	Molar flow of methanol in feed	mol/min
x	Conversion methanol	%
Activity	Activity of the catalyst	
m_{cat}	Catalyst mass	g
$A_{surf,\,cat}$	BET surface area of catalyst	g/m^2
t	Reaction time	min

4 Results

Relevant but also deviating results of synthesised and tested catalysts are presented in this section. More details about the experiments can be found in Appendix D-G. In Appendix B preparation experiments are presented.

4.1 Catalysts synthesis

In this section the results regarding reduction of precursors are presented.

From experiment RR01:T1 and RR01:T2 a heating rate of 5°C/min was assigned for further reduction experiments. These two experiments are not presented in XRD-graphs since the main reason for these experiments were to find a heating rate. All reduced samples showed spinel characteristics, they were black and magnetic.

4.1.1 Present phases (X-ray diffraction, XRD)

The samples that contained highest fractions of spinel were R01-SD-C2, R01-SD-C1 and R01-P-C1. The XRD-scans of these samples can be seen in Figure 4.1-4.4 and the non-spinel peaks are indicated: $Fe_2Mo_3O_8$ with circles, α-Fe_2O_3 with squares and MoO_2 with triangles. Traces of $Fe_2Mo_3O_8$ were present in RR02:G3 and R02-SD-C2, while R01-SD-C3, R01-P-C3, R02-SD-C3:1 and R02-SD-C3:2 seemed to contain higher amounts of this by-product. The only catalyst where α-Fe_2O_3 and MoO_2 were detected in was RR02:G1 which had been reduced in a low-water environment. In Table 4.1 the reduction specifications used for synthesis and the identified phases of each catalyst are presented.

Table 4.1. Identified phases in synthesised catalysts and synthesis conditions.

Catalyst	Catalyst specifications	Reduction specifications	Main phase	Additional phases
RR02:G1	Spray dried $Fe_{2.4}Mo_{0.6}$	H_2O content: 3.03 vol% Temperature: 480 °C	Spinel	α-Fe_2O_3 MoO_2
RR02:G3	Spray dried $Fe_{2.4}Mo_{0.6}$	H_2O content: 40 vol% Temperature: 480 °C	Spinel	$Fe_2Mo_3O_8$
R01-SD-C1	Spray dried $Fe_{2.7}Mo_{0.3}$	H_2O content: 22.41 vol% Temperature: 480 °C	Spinel	-
R01-SD-C2	Spray dried $Fe_{2.4}Mo_{0.6}$	H_2O content: 22.41 vol% Temperature: 480 °C	Spinel	-
R01-SD-C3	Spray dried Fe_2Mo_1	H_2O content: 22.41 vol% Temperature: 480 °C	Spinel	$Fe_2Mo_3O_8$
R01-P-C1	Precipitated $Fe_{2.7}Mo_{0.3}$	H_2O content: 22.41 vol% Temperature: 480 °C	Spinel	-
R01-P-C2	Precipitated $Fe_{2.4}Mo_{0.6}$	H_2O content: 22.41 vol% Temperature: 480 °C	Spinel	$Fe_2Mo_3O_8$
R01-P-C3	Precipitated Fe_2Mo_1	H_2O content: 22.41 vol% Temperature: 480 °C	Spinel	$Fe_2Mo_3O_8$
R02-SD-C2	Spray dried $Fe_{2.4}Mo_{0.6}$	H_2O content: 22.41 vol% Temperature: 480 °C (inert heating)	Spinel	$Fe_2Mo_3O_8$
R02-SD-C3:1	Spray dried Fe_2Mo_1	H_2O content: 3.03 vol% Temperature: 530 °C (inert heating)	Spinel	$Fe_2Mo_3O_8$
R02-SD-C3:2	Spray dried Fe_2Mo_1	H_2O content: 22.41 vol% Temperature: 530 °C (inert heating)	Spinel	$Fe_2Mo_3O_8$

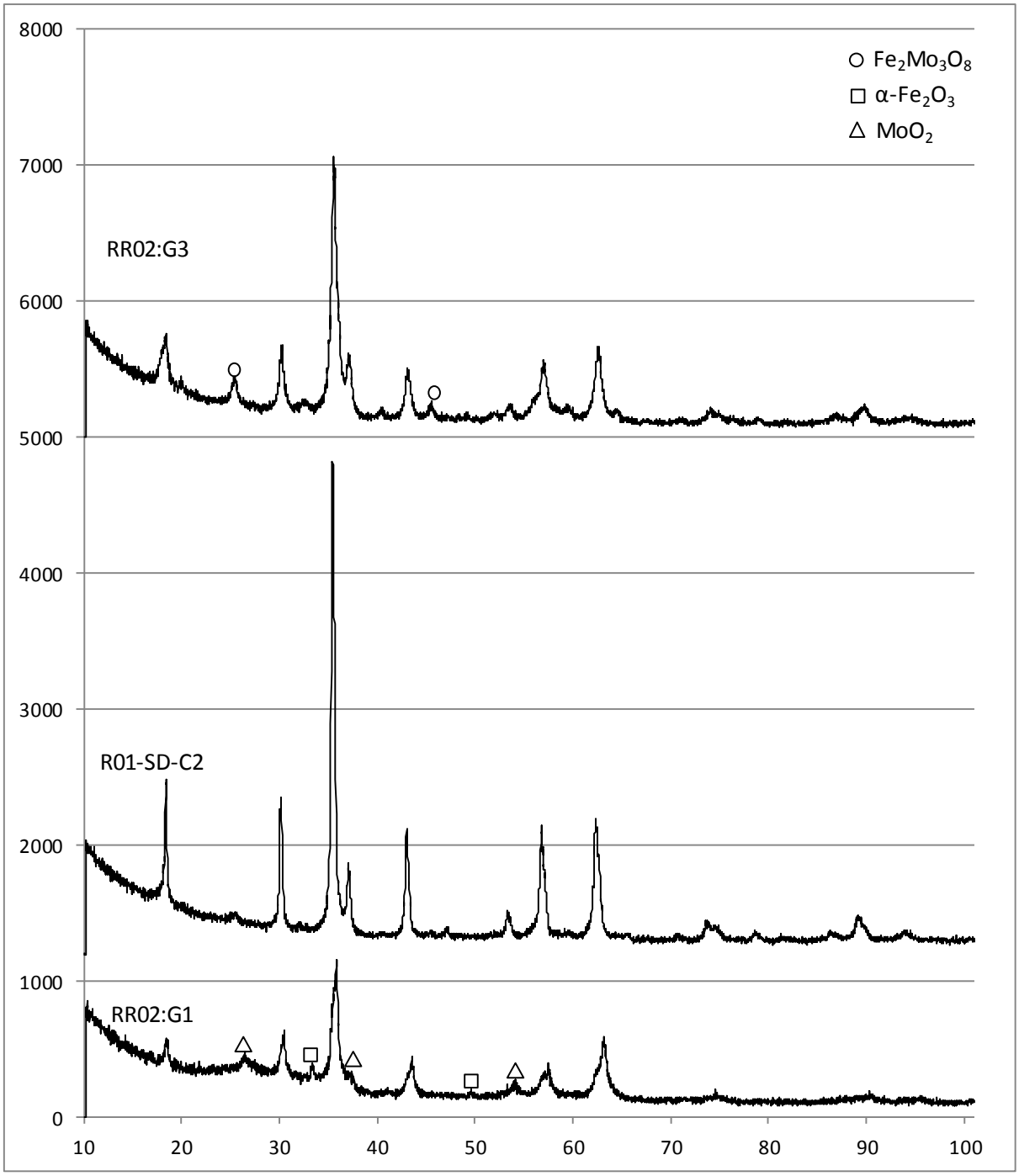

Figure 4.1. XRD-scan of spray dried spinels with Mo/Fe ratio 0.6/2.4 reduced in varying water content environments.

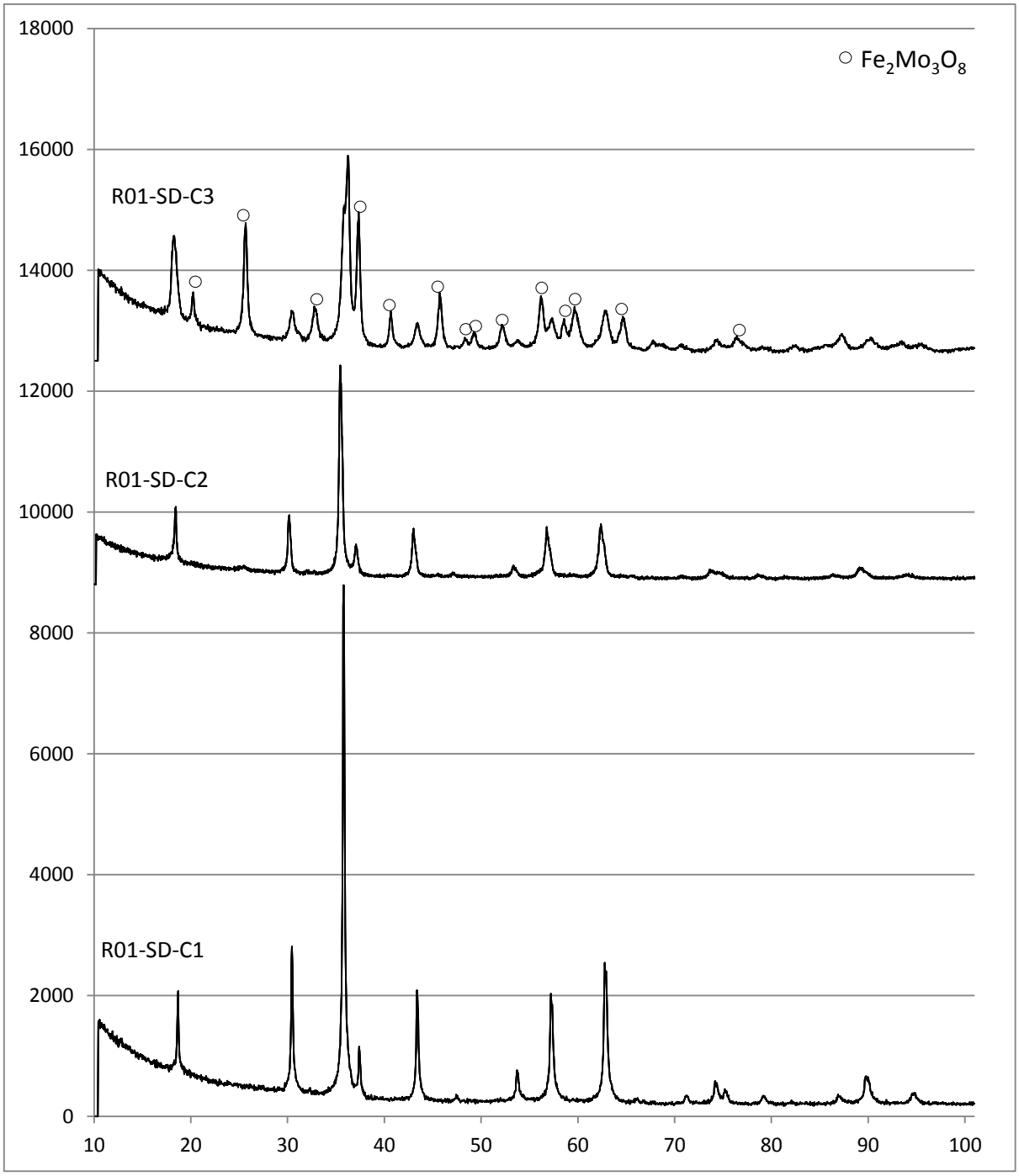

Figure 4.2. XRD-scan of spray dried spinels with different Mo/Fe ratios reduced under same conditions.

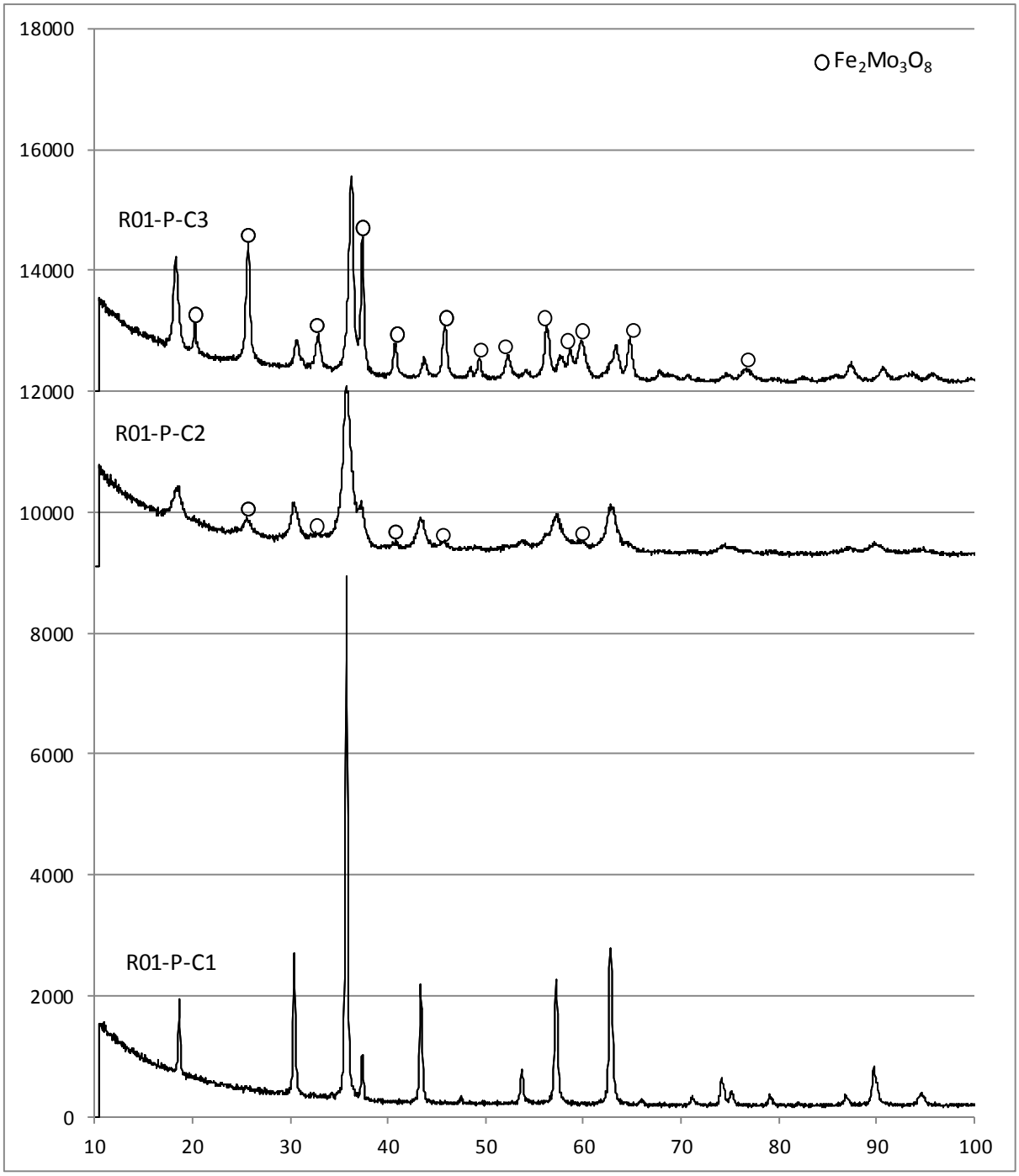

Figure 4.3. XRD-scan of precipitated spinels with different Mo/Fe ratios reduced under same conditions.

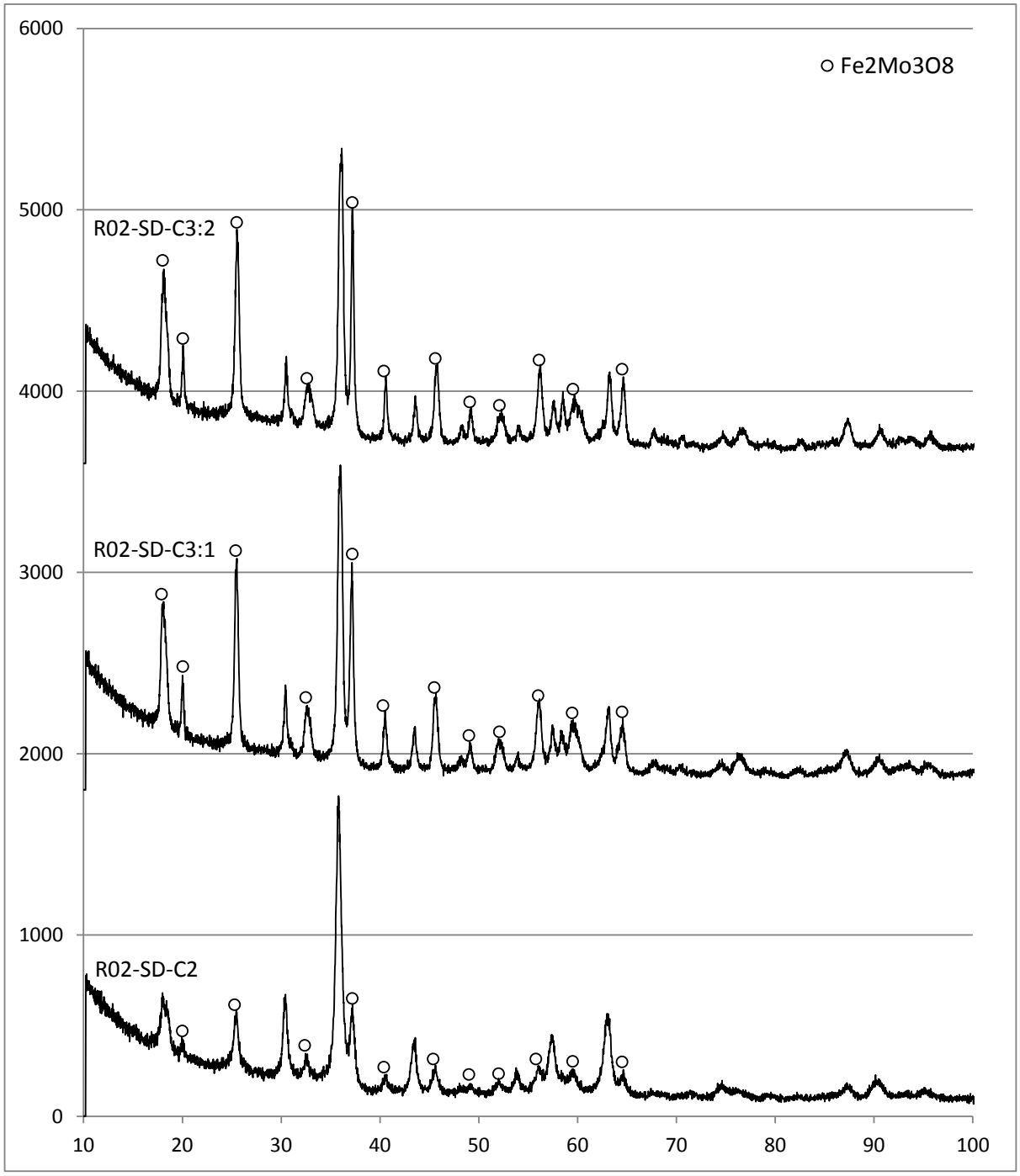

Figure 4.4. XRD-scan of spray dried spinels reduced under different conditions.

4.1.2 Specific surface (BET-analysis)

All BET surfaces before methanol oxidation can be seen in Table 4.2 below. All spinels except for R02-SD-C3:1 and R01-SD-C3:2, had specific surfaces in the interval 17-24m^2/g. No BET-analysis was made on RR02:T1 or RR02:T2 since traces of quartz in those samples could damage the equipment. Also, no BET-analysis was made on R02-SD-C2 due to lack of time.

Table 4.2. Specifications and BET-surfaces of fresh synthesised spinels.

Catalyst	Specification spinel	Surface (m^2/g)
RR02:G1	Spray dried, $Fe_{2.4}Mo_{0.6}$	17.98
RR02:G3	Spray dried, $Fe_{2.4}Mo_{0.6}$	22.14
R01-SD-C1	Spray dried, $Fe_{2.7}Mo_{0.3}$	23.52
R01-SD-C2	Spray dried, $Fe_{2.4}Mo_{0.6}$	19.28
R01-SD-C3	Spray dried, Fe_2Mo_1	19.47
R01-P-C1	Precipitated, $Fe_{2.7}Mo_{0.3}$	23.82
R01-P-C2	Precipitated, $Fe_{2.4}Mo_{0.6}$	22.27
R01-P-C3	Precipitated, Fe_2Mo_1	17.05
R02-SD-C3:1	Spray dried, Fe_2Mo_1	9.45
R02-SD-C3:2	Spray dried, Fe_2Mo_1	12.26

4.2 Catalytic performance

In this section the results of the catalytic performance are concluded; only important and deviating results are presented. Selectivity formaldehyde (FA) equivalent is the DMM selectivity added to FA selectivity and this selectivity is further used since 99% of the DMM is converted to formaldehyde at higher conversions. The concept of selectivity is defined in section 2.4. All used reference data can be seen in Appendix F and the activity reference data are based on the reference stability test during the first 3 hours.

4.2.1 Activity measurements

The activity of the spinels varied from 0.995-2.33 μmol/m^2/s for 300°C, which can be seen in Table 4.3 and 4.5. Figure 4.5 shows the CO selectivity as a function of methanol conversion and how it varies for different catalysts at 300°C. The figure shows that the spinels tend to form more CO than the reference catalyst. The selectivity toward product and by-products for each catalysts corresponding to activity data in Table 4.3 and 4.5 are shown in Table 4.4 and 4.6 respectively. Table 4.7 and 4.8 shows results from the activity tests when the reaction temperature was set to 330°C.

Table 4.3. Data from activity tests of R01-SD-C2 when the loading mass was varied and the reaction temperature was set to 300°C.

Catalyst	**R01-SD-C2**		
Mass catalyst (mg)	104.2	201.6	297.7
Conversion (%)	12.3	22.2	42.2
Selectivity FA (%)	86.6	82.2	82.3
Selectivity FA eq. (%)	92.54	86.3	86.02
BET-surface (m^2/g)	19.28	19.28	19.28
Activity (µmol/m^2/s)	1.94	1.84	2.33
Activity (µmol/g/s)	37.40	35.49	44.86

Table 4.4. Product profile from activity tests of R01-SD-C2 when the loading mass was varied and reaction temperature was set to 300°C, corresponding to Table 4.3.

Catalyst	**R01-SD-C2**		
FA	86.60	82.20	82.30
DME	6.19	7.29	8.33
DMM	5.93	4.1	3.68
CO	0.26	0.91	1.23
CO_2	0.01	0.01	0.01
MF	1.00	5.47	4.41
FA eq.	92.54	86.30	86.02

Table 4.5. Data from activity tests of different catalysts when reaction temperature was set to 300°C.

Catalyst	**R01-SD-C1**	**R01-P-C1**	**R02-SD-C3:1**
Mass catalyst (mg)	127.3	102.8	209.3
Conversion (%)	9.90	7.40	12.60
Selectivity FA (%)	72.40	5.50	84.60
Selectivity FA eq. (%)	78.53	9.51	89.91
BET-surface (m^2/g)	23.52	23.82	9.45
Activity (µmol/m^2/s)	1.06	0.995	2.04
Activity (µmol/g/s)	24.93	23.70	19.30

Table 4.6. Product profile from activity tests of different catalysts when reaction temperature was set to 300°C, corresponding to Table 4.5.

Catalyst	**R01-SD-C1**	**R01-P-C1**	**R02-SD-C3:1**
FA	72.40	5.50	84.60
DME	14.30	82.51	8.35
DMM	6.13	3.99	5.30
CO	1.02	2.66	0.31
CO_2	0.01	0	0.01
MF	6.13	5.32	1.42
FA eq.	78.53	9.51	89.91

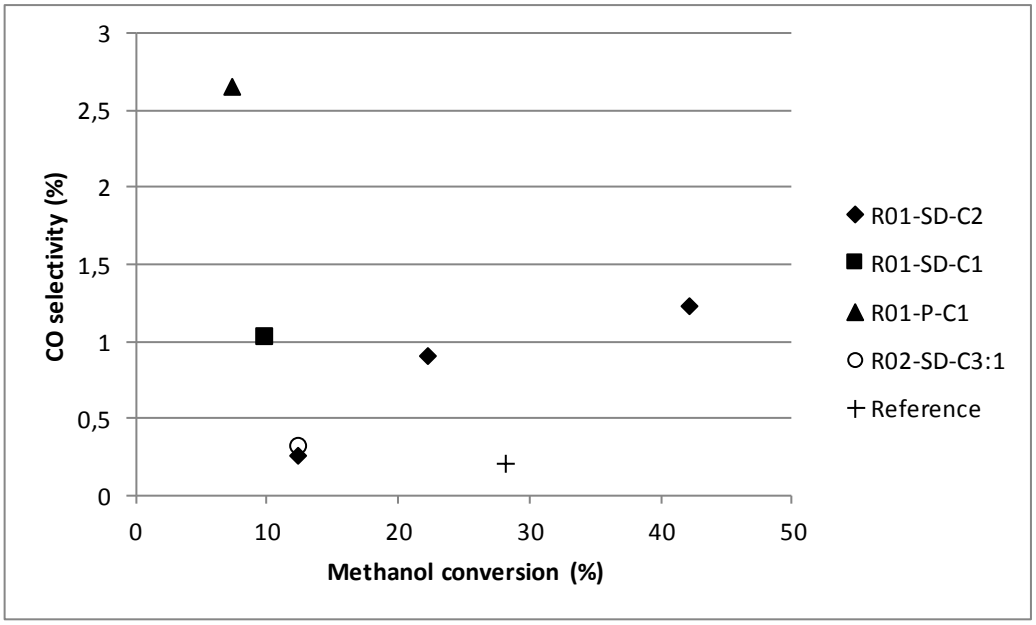

Figure 4.5. CO selectivity at different methanol conversions for different catalysts when the reaction temperature was set to 300°C, loading mass was 1g and GHSV was 38000 h^{-1}.

Table 4.7. Data from activity tests of different catalysts when reaction temperature was set to 330°C.

Catalyst	**R01-SD-C2**		**R01-SD-C1**	**R01-P-C1**	**R02-SD-C3:1**
Mass catalyst (mg)	104.2	201.6	127.3	102.8	209.3
Conversion (%)	36.10	77.8	52.00	22.80	32.70
Selectivity FA (%)	88.00	92.3	88.3	52.70	88.20
Selectivity FA eq. (%)	93.18	93.1	90.66	55.32	91.82
BET-surface (m^2/g)	19.28	19.28	23.52	23.82	9.45
Activity (µmol/m^2/s)	5.70	6.439	5.59	3.04	5.30
Activity (µmol/g/s)	109.89	124.13	131.37	72.42	50.05

Table 4.8. Product profile from activity tests of different catalysts when reaction temperature was set to 330°C, corresponding to Table 4.7..

Catalyst	**R01-SD-C2**		**R01-SD-C1**	**R01-P-C1**	**R02-SD-C3:1**
FA	88.00	92.30	88.30	52.70	88.20
DME	5.29	3.48	5.14	35.04	6.44
DMM	5.41	0.80	2.37	2.63	3.66
CO	0.78	2.34	1.03	3.07	0.53
CO_2	0.01	0.01	0.01	0.01	0.01
MF	0.74	1.07	3.16	6.57	1.20
FA eq.	93.18	93.1	90.66	55.32	91.82

4.2.2 Stability and ageing

An ageing test was performed on spinel R01-SD-C2 since this spinel showed promising activity results, Table 4.3 in section 4.2.1. In Figure 4.6 results from the stability test are presented together with a reference catalyst.

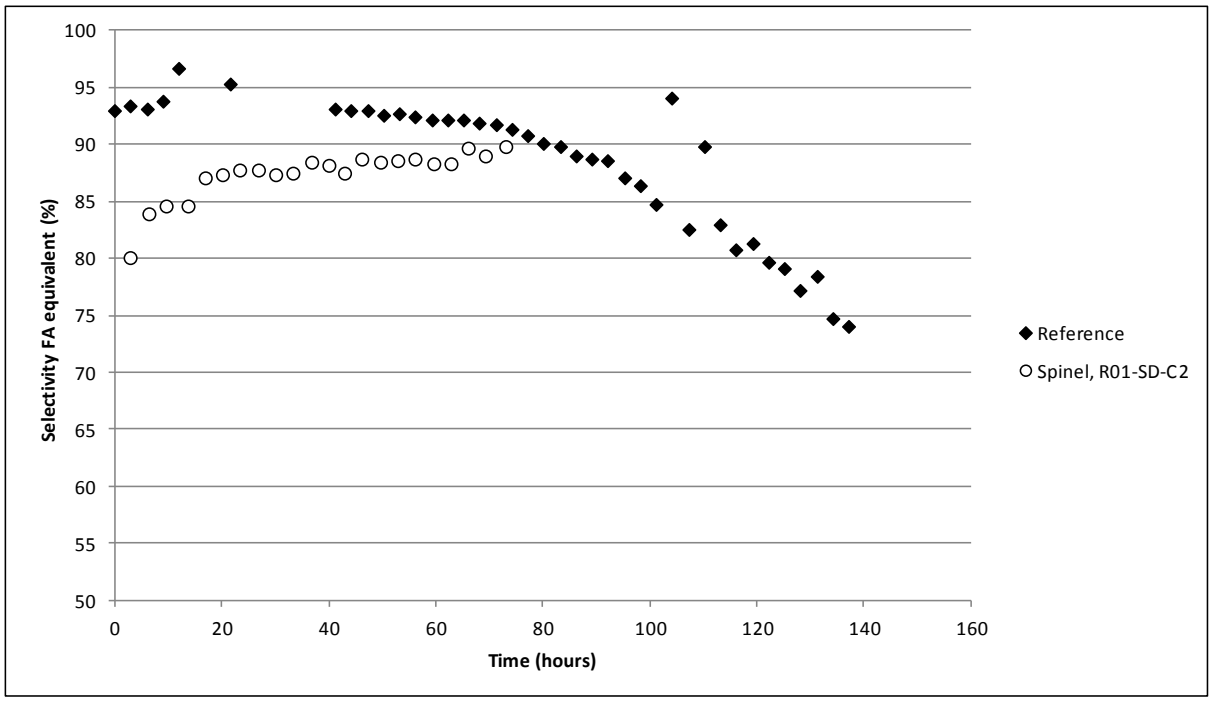

Figure 4.6. The FA equivalent selectivity of a reference catalyst and R01-SD-C2 varying over time when the reaction temperature was set to 300°C.

The spinel that were analysed by ICP-AES and its corresponding result are presented in Table 4.9 below. All stability data can be found in Appendix E and F while all ICP-analysis data is found in Appendix G.

Table 4.9. Ratio Mo/Fe in fresh and aged catalysts.

		Ratio Mo/Fe	
Catalyst		Theoretical	Measured
R01-SD-C2	Fresh	0.25	0.261
(Stability test)	Aged		0.266

5 Discussion

5.1 Catalyst synthesis

All synthesised catalysts contained the spinel phase in different amounts, but only 3 of the attempted synthesis experiments resulted in pure spinel phase. In Table 4.1 all catalysts and identified phases are presented. From the XRD-analysis, Figure 4.1-4.4, it was found that higher fractions of molybdenum present in the precursor generated more $Fe_2Mo_3O_8$ during reduction at 480°C. While R01-SD-C1 showed no evidence of containing $Fe_2Mo_3O_8$, the XRD graph of R01-SD-C3 showed several significant Fe_2Mo_3O peaks, see Figure 4.2. The spray dried sample where the Mo/Fe ratio is 0.6/2.4, R01-SD-C2, seemed to be almost pure; only low-intense peaks of $Fe_2Mo_3O_8$ were recognised in the XRD-scan. It seems as if the iron molybdenum precursor tends to form the slightly more oxidised phase $Fe_2Mo_3O_8$ if a higher amount of molybdenum is present and when the Mo-content is low, the spinel synthesis is less sensitive to varying reduction conditions.

The only catalyst prepared by precipitation that was completely pure spinel phase after reduction, was the one with lowest Mo-content, R01-P-C1. The XRD-scan of spinel R01-P-C2 contained some low intense peaks of $Fe_2Mo_3O_8$ while for R01-P-C3, as was the case for the corresponding spray dried spinel, several $Fe_2Mo_3O_8$-peaks were discovered in the XRD-scan. However, since the spray dried spinel with Mo/Fe ratio 0.6/2.4 had higher fraction of spinel phase than the corresponding precipitated spinel, this shows that the spray dried spinels are slightly easier to synthesise. A possible reason for this is that the precipitated spinels contain more impurities from the precursor synthesis. This can affect the formation of spinel structure during reduction if the temperature is increased too fast.

As explained above, the spinels with the highest molybdenum content (C3, see section 3.1 for denominations) formed higher amounts of $Fe_2Mo_3O_8$ during reduction than spinels with lower contents of Mo. A possible explanation for this is that higher molybdenum contents might affect the accessibility to reduce the sample, and more hydrogen or less water is needed to reduce the sample and form higher amounts of the spinel phase. To investigate this further, a reduction of the precursor with high Mo-content at higher temperature and lower water content in the reducing gas was performed, R02-SD-C3:1. Unfortunately, the XRD-scan of this spinel still showed high content of $Fe_2Mo_3O_8$. Moreover, the BET-surface was significantly lower for this spinel which was also the case for the other spinel that was reduced at a higher temperature, R02-SD-C3:2. This could be the effect from high contents of other phases that are present and these other phases might have lower specific surfaces. Another possible explanation is the fast temperature increase of the spinel; both R02-SD-C3:1 and R02-SD-C3:2 were heated inertly and the heating rate of the catalyst precursors was much higher than in other reductions, approximately 20°C/min. The reduced surface area could also be the result of rapid oxidation which causes the surface to sinter, but since all spinels were oxidised in a controlled way after reduction, this is not likely. Even though that R02-SD-C3:1 contained $Fe_2Mo_3O_8$, the activity test of this spinel still showed results that were as good as for catalyst R01-SD-C2, but this is further discussed in section 5.2.1 below.

An additional result indicating that slow heating of the material is needed or/and reduction should start at lower temperatures, is when comparing R01-SD-C2 and R02-SD-C2. The XRD-graph of R01-SD-C2 showed basically a pure spinel phase while the XRD-graph of R02-SD-C2 actually contained some low-intense peaks of $Fe_2Mo_3O_8$, Figure 4.2 and 4.4 respectively. The only difference between the two catalysts was the temperature increase during or before reduction. Inert heating (catalyst heating when no H_2 is present) was applied on spinel R02-SD-C2 with approximately heating rate 20°C/min, while a controlled heating rate of 5°C/min from 250 to 480°C was used for the reduction of R01-SD-C2. In [24], it was also found that the intensity of the $Fe_2Mo_3O_8$-peaks is affected by the temperature, at least for the spinels with higher Mo-content.

The only spinel that contained other undesired phases than $Fe_2Mo_3O_8$ was RR02:G1, which contained α-Fe_2O_3 and MoO_2. This spinel was one out of two spinels that were reduced in a low water environment. The other spinel reduced in the same water content was R02-SD-C3:1 but the only phases present in R02-SD-C3:1 were spinel and $Fe_2Mo_3O_8$. Potentially this means that RR02:G1, which contained less Mo, required more water while R02-SD-C3:1 required less water or more hydrogen to favour the spinel phase. R02-SD-C3:2, which was reduced in the same manner as R02-SD-C3:1 but in higher water content, also contained high intense peaks of $Fe_2Mo_3O_8$ which is again indicates that less water is needed for higher Mo contents.

It should also be mentioned that XRD-analysis is not an accurate method to quantify the different phases but the varying intensity of the peaks still gives a hint of the amount. Obviously high intense peaks indicate higher fractions and low intense peaks indicate lower fractions. The method also tells if undesired phases are formed and this also gives an indication of at which conditions the spinel phase is favoured.

The spray dried material was for practical reasons hard to work with; the small particles got stuck on surfaces that caused cleaning difficulties. When performing experiments, pressure complications arose even when the particles were tableted and sieved; the pressure drops over the catalyst bed were significant, approximately 0.5-3 bar. The precipitated particles were a bit easier to manage since the particles were not as easily crumbled into fine powder. When synthesising and working with spray dried spinels in the future, an adhesive should be used when tableting the particles. This could prevent complications with pressure drop and particle escape from the catalyst bed.

5.2 Catalytic performance

5.2.1 Activity

Activity measurements were performed on several spinels and the formaldehyde equivalent selectivity of these spinels varied from 78 to 93% at 300°C except for R01-P-C1, which showed a much lower selectivity to formaldehyde, approximately 10%. This is lower than for the commercial catalyst used today, and the reference catalyst also accounted for the highest formaldehyde equivalent selectivity. In Figure 5.1 the selectivity to formaldehyde equivalents at given conversion and catalyst is presented. As mentioned above and as the figure displays, R01-P-C1 showed very poor selectivity while R01-SD-C2 showed almost as high selectivity as the reference, however, at low conversion. Formaldehyde selectivity of R01-SD-C2 at the two higher conversions was in fact lower. The difference in outcome even though it is the exact same spinel, could simply be because of the difference in conversion rate. It could also imply that some kind of temperature activation occurs; the catalysts were actually heated different amount of time before the activity tests. R01-SD-C2 at lowest conversion was heated the longest time before the activity test and it also showed highest selectivity, Figure 5.1. The ageing test also showed similar behaviour, an activation of the catalyst over time was recognised which resulted in formaldehyde equivalent selectivity at 89%. Something happens with the structure and the catalyst surface, probably that Mo is transported to the surface when it is exposed to heat which activates the catalyst and increase catalyst activity and formaldehyde selectivity.

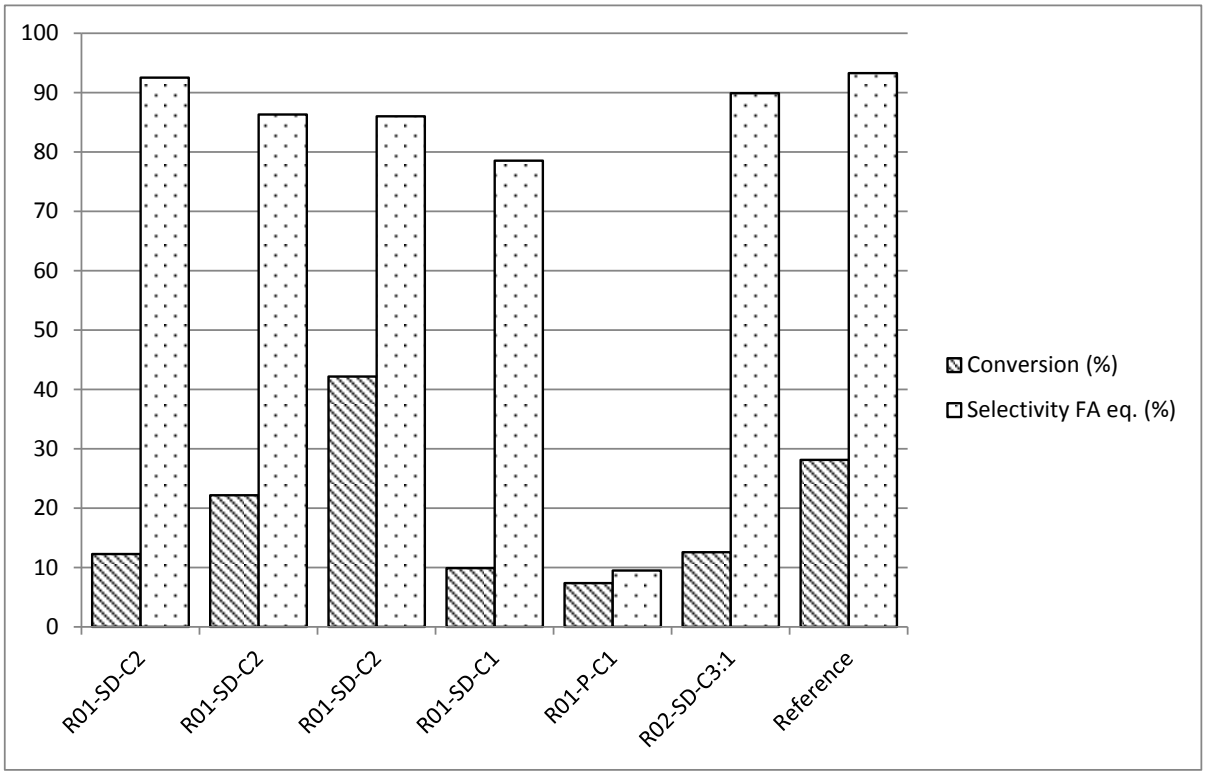

Figure 5.1. Conclusion of the activity results where selectivity toward formaldehyde equivalents is shown for each catalyst at given conversion when the reaction temperature was set to 300°C. The figure corresponds to Table 4.3 and 4.5 in section 4.2.1.

Another interesting activity result that is worth to mention is the selectivity toward CO_2 and CO. The selectivity to CO_2 seemed to be lower during methanol oxidation than during bypass which would imply that the CO_2 is consumed. At the same time, the CO selectivity is increasing. A possible explanation for this is that the gas chromatograph could not completely separate the peaks of CO_2 and CO which would give peak areas that are incorrect. A too high and too low selectivity toward CO and CO_2 respectively is a possible outcome of this. However, the CO formation from reaction over the spinels is still higher than for the reference catalyst and highest CO formation is observed for the spinel with lowest Mo-content and highest Fe-content, see Figure 4.5. This is an expected result since iron promote oxidation of formaldehyde (see reac. 3.5 and 3.6 in section 3.5) and hence CO and CO_2 formation. Clearly this is an issue with the catalytic performance of the spinel, but the results also showed that when more Mo is present in the catalyst, less CO will form. Catalyst R01-SD-C2 and R02-SD-C3:1 showed lowest CO selectivity of the spinels but R02-SD-C3:1 was not pure spinel phase. Therefore would it be interesting to find out if a pure spinel with Mo/Fe ratio 1/2 would form even less CO. This is further discussed in Future work.

As mentioned above, the spinels with Mo/Fe ratio 0.3/2.7 that were the least difficult catalysts to synthesise showed poor activity results. This was the case for both the precipitated and the spray dried spinel and the precipitated showed very high DME selectivity, roughly 83%. Activity measurements were performed on R01-SD-C1 for investigation of higher conversion rates and the results are only shown in Figure 9.2 in Appendix D and not in the result. As can be seen in the figure, the methanol outlet concentration suddenly drops and the CO outlet concentration increase. Obviously more formaldehyde is also formed, but the sudden change in conversion indicates that the catalyst is undergoing some kind of surface transformation. The increase of CO selectivity could be the result of molybdenum lost; but this is not likely since the ICP-analysis of this catalyst, see Appendix G, showed that the ratio Mo/Fe rather increased than decreased after reaction. Instead a cluster of iron at the surface could be the reason to the rapid change in methanol conversion. The phenomenon was not seen neither when activity nor stability test was performed on R01-SD-C2 which implies that higher Mo content than for C1 is needed to have sufficient Mo segregating from bulk to surface. Again, a pure spinel with Mo/Fe ratio 1/2 would be interesting to use for activity measurements.

When the reaction temperature was set to 330°C, the selectivity to formaldehyde was higher and selectivity to DME was lower for all catalysts. This was an expected outcome since this is also seen when performing activity tests on the commercial catalyst. As the conversion also increased, the CO selectivity increased as well. All activity tests of the spinels except for R01-P-C1 gave formaldehyde selectivities above 90%, see Figure 5.2.

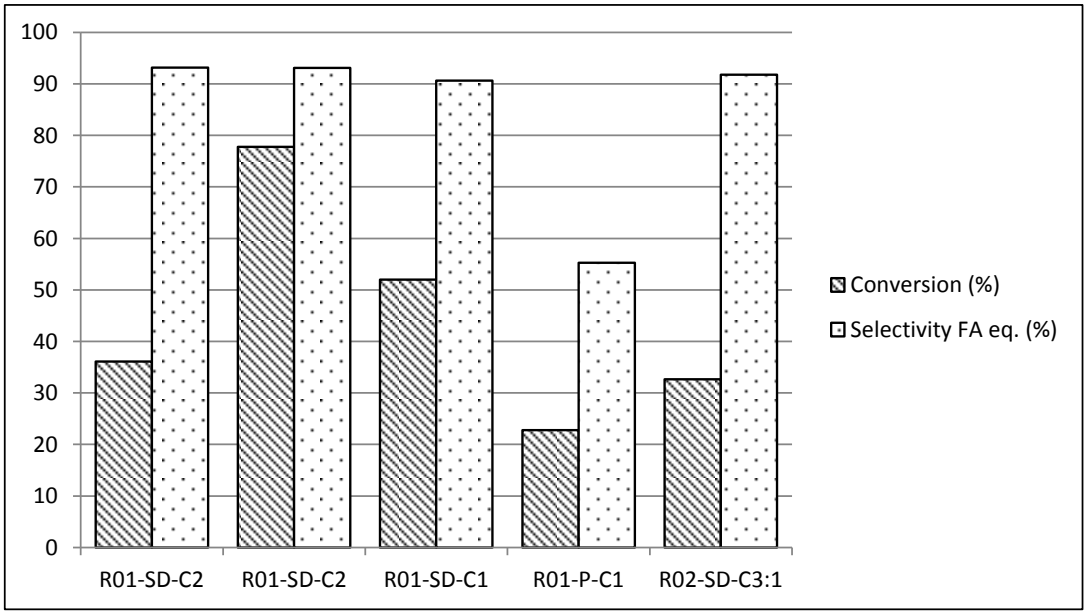

Figure 5.2. Conclusion of the activity results where selectivity toward formaldehyde equivalents is shown for each catalyst at given conversion when the reaction temperature was set to 330°C. The figure corresponds to Table 4.7 in section 4.2.1.

5.2.2 Stability and ageing

The stability test that was performed on R01-SD-C2 showed catalyst activation over time; the conversion increased from 34 to 86% and the activity from 2.51 to 5.63μmol/m^2/s, see Appendix E. This is compared to the commercial catalyst which rather shows deactivation over the same amount of time, see Figure 4.6. Since the CO and CO_2 formation also increase over time (even though the CO_2-increase is small), this could imply that iron is assembled at the catalyst surface, resulting in that produced formaldehyde will further oxidise to CO and CO_2 (see reac. 3.1-3.6 for possible methanol oxidation reactions). However, the selectivity toward formaldehyde equivalents increases from 78% to 90% and this rather implies that the catalyst, as mentioned above in section 5.2.1, simply is activated by temperature; Mo segregates to the surface. The Mo on the surface provides with formaldehyde selectivity, which is discussed under section 7.

The high activation of the catalyst was a bit unexpected; in [24] the activity of a catalyst with similar preparation technique showed overall deactivation over time. On the other hand, this catalyst had a Mo/Fe ratio of 0.071 which is significantly lower than for R01-SD-C2 which has the Mo/Fe ratio 0.25. Moreover, the surface area after the ageing test of R01-SD-C2 was not established in this project and the activity calculations are hence not completely trustworthy since they are based on the fresh catalyst surface area. However, since the catalyst conversion and selectivity increased and these concepts are not based on catalyst surface area, it is most likely that the activity actually increase as well.

The ICP-analysis of fresh and spent catalyst showed an increase of molybdenum after reaction for both of the two catalysts that were analysed, see Appendix G. It would have been desirable to perform an atomic absorption spectroscopy to confirm these results since an ICP-analysis is not completely trustworthy. However, even though the quantity is not entirely correct, the ICP-result still shows that the ratios before are similar to the ratios after reaction which indicates that the catalysts at least do not lose molybdenum. It should also be noted that R01-SD-C1 during the activity test was subjected to 330°C and still shows promising stability properties; no Mo is lost.

6 Conclusions

Some conclusions can be made from this master thesis project which are presented in this section.

A higher level of understanding of how Fe-Mo-oxides with different Mo-content react in a H_2/H_2O environment was established. The spinels with a lower Mo-content were easier to synthesise; the heating rate and ratio H_2/H_2O did not particularly affect the outcome of the purity of these spinels. At higher Mo-content however, the temperature and other reduction conditions seem to play a more significant part and the formation of spinel phase is more sensitive. The synthesised spinels of higher Mo-content also contained higher amount of the unwanted phase $Fe_2Mo_3O_8$. Also, the spray dried material showed better results than the precipitated both regarding synthesis accessibility and catalytic performance.

The activity and stability measurements showed that the spinels are activated over time which indicates that Mo segregates to the surface. The formaldehyde selectivity is however lower for the spinel than for the reference catalyst. No molybdenum was lost during the stability test which shows that even though that Mo diffuses to the surface, the structure is still maintained. This is a promising catalyst quality and if the selectivity can be improved, this catalyst can provide higher phase stability and longer lifetime.

7 Future work

There are some improvements of the catalysts that can be implemented. Firstly, investigate how to synthesise a spinel with iron molybdenum ratio 2:1 and perform activity and stability measurements. The results in this reports show that higher molybdenum content yields higher formaldehyde equivalent selectivity and lower CO formation. A spinel with high molybdenum content would consequently be interesting to synthesise to improve the product selectivity. To learn at what conditions the spinels with higher Mo-content can be synthesised, experiments should be performed where the conditions are varied as the content spinel phase is quantified simultaneously. Parameters that would be interesting to look at and vary would be the synthesis temperature and the ratio hydrogen/water in the reduction gas. Looking at the phase diagram for an iron spinel, Figure 2.4, the spinel phase is promoted at lower temperatures. Consequently, a more extensive analysis at what temperatures the spinel is starting to synthesise during reduction is required. High temperatures such as 700°C could also be interesting to attempt since several studies that have synthesised spinels by this method have performed the reduction at temperatures around 700°C [21, 26]. The results in this report also demonstrated that heating rate affect the outcome of the spinel phase purity and thus, this is definitely something to consider and investigate when synthesising the spinels.

Synthesised catalysts should then be studied in terms of stability tests to investigate if the catalyst is activated as R01-SD-C2 was in this report. Several stability tests, over different amount of time periods should be performed together with surface characterisation as has been done in other studies [36]. This would give a more extensive and solid analysis since conclusions of how the catalyst structure and surface is affected over time can be made. A few different reaction temperatures should also be examined to determine how well the catalyst is performing at higher temperatures over time.

To synthesise a spinel with a higher Mo content, an alternative could be to attempt reduction by CO_2/CO or a different synthesis technique. Using CO_2/CO for reduction, complications concerning water vaporisation would be eliminated which enables slow heating rates from room temperature. Using a different synthesis technique would possibly facilitate the synthesis of the spinels with higher Mo-content. In [37] spinels were successfully synthesised by oxidation of a suspension and the Mo-ferrite that was formed had a Mo/Fe ratio of 0.39 and the XRD-scan showed a pure phase spinel. It could hence be interesting to try to mimic the catalyst synthesis in this report to synthesise spinels of higher Mo-contents. Also in [24] pure spinel phase was formed when oxidisation of a suspension was applied on Mo/Fe ratios 0.071 and 0.2. In this report however, at higher Mo/Fe ratios the catalyst contained less spinel phase and more $Fe(MoO_4)$ and α-Fe_2O_3.

To improve the already successfully synthesised spinel from this report there are some suggestions. In has been shown that it is the Mo enrichment at the surface that gives the catalyst high selectivity and activity [38, 39, 40]. This was demonstrated by studying the surfaces of iron molybdenum catalysts, for example, an iron core impregnated with MoO_3. If MoO_3 coating could be applied on a spinel core by, for instance, the incipient wetness method,

the MoO_3 would obviously provide the spinel catalyst with a higher Mo-content and thus result in higher formaldehyde selectivity. Since the spinel structure in itself shows better stability properties, see section 4.2.1 and 4.2.2, the molybdenum layer would probably be intact for a longer time period than for an iron core but also than for the commercial catalyst used today. As it was succeeded to synthesise a pure phase spinel with Mo/Fe ratio 0.6/2.4 in this master thesis project, experiments where this spinel is synthesised and then impregnated with MoO_3 would be a reasonable start. The impregnation method is explained in several reports [38, 41]. In [41], an iron core was coated with a few MoO_3 layers to increase the surface area and doped with a small amount of Al to stabilise the surface area which also provides information of how the catalyst can be constructed.

Another potential improvement of the catalyst that is a bit more time consuming is to dope the spinel with a small amount of a different metal. This could potentially facilitate the synthesis of spinel phase and there are studies which this has been done. In [23] vanadium was substituted into the structure and the spinel was synthesised without complications. In [42] Co-Mo spinels were constructed and in [43] Mo-Ti-spinels of various metal ratios. In these studies it were not reported of any complications concerning synthesising the spinel phase.

8 References

[1] L.-O. Andersson, "Formaldehyde expected to grow beyond GDP globally," *Informally Speaking (newsletter from Johnson Matthey Formox),* p. 8, Autumn 2015.

[2] G. Reuss, W. Disteldorf, A. O. Gamer and A. Hilt, "Formaldehyde," in *Ullman's Encyclopedia of Industrial Chemistry*, Weinheim, Wiley-VCH Verlag GmbH & Co. KGaA, 2012, pp. 735-763.

[3] E. Söderhjelm, M. P. House, N. Cruise, J. Holmberg, M. Bowker, j.-O. Bovin and A. Andersson, "On the Synergy Effect in MoO_3-$Fe_2(MoO_4)_3$ Catalysts for Methanol Oxidation to Formaldehyde," *Topics in Cataysis,* vol. 50, p. 145–155, 2008.

[4] H. R. Gerberich and G. C. Seaman, "Formaldehyde," in *Kirk-Othmer Encyclopedia of Chemical Technology*, John Wiley & Sons, Inc., 2013, pp. 1-12.

[5] Fire Protection Guide on Hazardous Materials, Quincy: National Fire Protection Association, 1986, pp. 49-51.

[6] R. Spence and W. Wild, "The preparation of liquid monomeric formaldehyde," *J. of the Chemical Soc.*, vol. 506, pp. 338-340, 1935.

[7] A. Andersson, "How a fourfold productivity increase has been obtained," *Informally Speaking (newsletter from Johnson Matthey Formox),* pp. 14-17, Autumn 2015.

[8] C. N. Satterfield, "Catalytic Oxidation," in *Heterogeneous Catalysis in Industrial Practice*, McGraw-Hill, Inc, 1991, pp. 267-337.

[9] A. P. V. Soares, M. F. Portela and A. Kiennemann, "Methanol Selective Oxidation to Formaldehyde over Iron-Molybdate Catalysts," *Catalysis Reviews: Sci. and Eng.,* vol. 47, pp. 125-174, 2005.

[10] "Formox," Johnson Matthey, [Online]. Available: http://www.formox.com/formox-process. [Accessed 25 01 2016].

[11] C. N. Satterfield, "Introduction and Basic Concepts," in *Heterogeneous Catalysis in Industrial Practice*, McGraw-Hill, Inc, 1991, pp. 1-30.

[12] R. Häggblad, J. B. Wagner, S. Hansen and A. Andersson, "Oxidation of methanol to formaldehyde over a series of $Fe_{1-x}Al_x$-V-oxide catalysts," *J. of Catalysis,* vol. 258, pp. 345-355, 2008.

[13] M. Carbucicchio and F. Trifirò, “Surface and Bulk Redox Processes in Iron-Molybdate-Based Catalysts,” *J. of catalysis,* vol. 45, pp. 77-85, 1976.

[14] K. I. Ivanov∗ and D. Y. Dimitrov, “Deactivation of an industrial iron-molybdate catalyst for methanol oxidation,” *Catalysis Today,* vol. 154, p. 250–255, 2010.

[15] M. Bowker, R. Holroyd, M. House, R. Bracey, C. Bamroongwongdee, M. Shannon and A. Carley, “The Selective Oxidation of Methanol on Iron Molybdate Catalysts,” *Topics in Catalysis,* vol. 48, p. 158–165, 2008.

[16] W. L. Holstein and C. J. Machiels, “Inhibition of Methanol Oxidation by Water Vapor—Effect on Measured Kinetics and Relevance to the Mechanism,” *J. of Catalysis,* vol. 162, pp. 118-124, 1996.

[17] S. Deshmukh*, M. van Sint Annaland and J. Kuipers, “Kinetics of the partial oxidation of methanol over a Fe-Mo catalyst,” *Appl. Catalysis A: General,* vol. 289, pp. 240-255, 2005.

[18] H. Schubert, U. Tegtmeyer and R. Schlögl, “On the mechanism of the selective oxidation of methanol over elemental silver,” *Catalysis Lett.,* vol. 28, pp. 383-395, 1994.

[19] G. J. Millar, J. B. Metson, G. A. Bowmaker and R. P. Cooney, “In sifu Raman Studies of the Selective Oxidation of Methanol to Formaldehyde and Ethene to Ethylene Oxide on a Polycrystalline Silver Catalyst,” *J. of the Chemical Soc., Faraday Trans.,* vol. 91, no. 22, pp. 4149-4159, 1995.

[20] W.-K. Li, G.-D. Zhou and T. Mak, “Basic Inorganic Crystal Structures and Materials,” in *Advanced Structural Inorganic Chemistry,* New York, Oxford University Press, 2008.

[21] E. Kester, P. Perriat, B. Gillot, P. Tailhades and A. Rousset, “Correlation between oxidation states of transition metal ions and variation of the coercivity in mixed-valance defect spinel ferrites,” *Solid State Ionics,* Vols. 101-103, pp. 457-463, 1997.

[22] M. Massa, R. Häggblad, S. Hansen and A. Andersson, “Oxidation of methanol to formaldehyde on cation vacant Fe-V-Mo-oxide,” *Appl. Catalysis A: General,* vol. 408, pp. 63-72, 2011.

[23] R. Häggblad, S. Hansen, L. R. Wallenberg and A. Andersson, “Stability and performance of cation vacant $Fe_{3-x-y}V_{x\ y}O_4$ spinel phase catalysts in methanol oxidation,” *J. of catalysts,* vol. 276, pp. 24-37, 2010.

[24] V. Björk, “Metanoloxidation med järn-molybden-katalysatorer av spinellstruktur,” M.S. thesis, Dept. of Chemical Eng., Lund Univ., Lund, 2011.

[25] *Personal communication, Robert Häggblad, Catalyst R&D Manager at Johnson Matthey Formox AB,* Perstorp, 2016.

[26] B. Gillot and B. Domenichini, "Reactivity of the submicron molybdenum ferrites towards oxygen and formation of new cation deficient spinels," *Solid state ionics,* Vols. 63-65, pp. 620-627, 1993.

[27] M. V. Nikolenko, A. O. Kostynyuk, F. Goutenoire and Y. V. Kalashnikov, "Chemical Precipitaion of Iron(III) Molybdate + Molybdenum Mixtures through Continuous Crystallization," 2014.

[28] R. Häggblad, "Selective Oxidation over Mixed Metal Catalysts," Ph.D. dissertation, Dept. of Chemical Eng., 2010.

[29] B. Hou, H. Zhang, H. Li and Q. Zhu, "Study on Kinetics of Iron Oxide Reduction by Hydrogen," *Chinese J. of Chemical Eng.,* vol. 20, no. 1, pp. 10-17, 2012.

[30] S. Kaluza and M. Muhler, "A novel continuous approach for the synthesis and characterisation of pure and mixed metal oxide systems applied in heterogeneous catalysis," in *Scientific Bases for the Preparation of Heterogeneous Catalysts,* Louvain-la-Neuve, Elsevier, 2010, pp. 217-220.

[31] J. Kunert, A. Drochner, J. Ott, H. Vogel and H. Fuess, "Synthesis of Mo/V mixed oxide catalysts via crystallisation and spray drying - a novel approach for controlled preparation of acrolein to acrylic acid catalysts," *Appl. Catalysis A: Genera,* vol. 269, pp. 53-61, 2004.

[32] M. Le, J. Van Craenenbroeck, I. Van Driessche and S. Hoste, "Bismuth molybdate catalysts synthesized using spray drying for the selective oxidation of propylene," *Appl. Catalysis A: General,* vol. 249, pp. 355-364, 2003.

[33] C. Martos, J. Dufour and A. Ruiz, "Synthesis of Fe_3O_4-based catalysts for the high-temperature water gas shift reaction," *Int. J. of hydrogen energy,* vol. 32, pp. 44476-4481, 2009.

[34] J. Dufour, C. Martos, A. Ruiz, M. Maroño and J. Sánchez, "Synthesis of copper promoted high temperature water-gas shift catalysts by oxidation-precipitation," *Int. J. of hydrogen energy,* vol. 39, pp. 17600-17607, 2014.

[35] G. Ertl, H. Knözinger and J. Weitkamp, Preparation of Solid Catalysts, Weinhem: Wiley-VCH, 1999, pp. 128-129.

[36] C. Brookes, M. Bowker, E. K. Gibson, D. Gianolio, K. M. Mohammed, S. Parry, S. M. Rogers, I. P. Silverwood and P. P. Wells, "In situ spectroscopic investigations of MoO_x/Fe_2O_3 catalysts for the selective oxidation of methanol," *Catal. Sci. Technol.*, vol. 6, pp. 722-730, 2016.

[37] B. P. Hahn, J. W. Long, A. N. Mansour, K. A. Pettigrew, M. S. Osofsky and D. R. Rolison, "Electrochemical Li-ion storage in defect spinel iron oxides: the critical role of cation vacancies," *Energy Environ. Sci.*, vol. 4, pp. 1495-1502, 2011.

[38] M. P. House, M. D. Shannon and M. Bowker, "Surface Segregation in Iron Molybdate Catalysts," *Catalysis Lett.*, vol. 122, pp. 210-213, 2008.

[39] B. R. Yeo, G. J. Pudge, K. G. Bugler, A. V. Rushby, S. Kondrat, J. Bartley, S. Golunski, S. H. Taylor, E. Gibson, P. P. Wells, C. Brookes, M. Bowker and G. J. Hutchings, "The surface of iron molybdate catalysts used for the selective oxidation of methanol," *Surface Sci.*, vol. 648, pp. 153-169, 2016.

[40] C. Brookes, P. P. Wells, G. Cibin, N. Dimitratos, W. Jones, D. J. Morgan and M. Bowker, "Molybdenum Oxide on Fe_2O_3 Core-Shell Catalysts: Probing the Nature of the Structural Motifs Responsible for Methanol Oxidation Catalysis," *ACS Catalysis*, vol. 4, pp. 243-250, 2014.

[41] S. Chapman, C. Brookes, M. Bowker, E. K. Gibson and P. P. Wells, "Design and stabilisation of a high area iron molybdate surface for the selective oxidation of methanol to formaldehyde," *Faraday Discussions*, 2015.

[42] Z. Heiba, N. Y. Mostafa and O. H. Abd-Elkander, "Structura land magnetic properties correlated with cation distribution of Mo-substituted cobalt ferrite nanoparticles," *J. of Magnetism and Magnetic Materials*, vol. 368, pp. 246-251, 2014.

[43] A. Roy and J. Ghose, "Studies on Some Titanium-Substituted Fe_2MoO_4 Spinel Oxides," *J. of solid state chemistry*, vol. 140, pp. 56-61, 1998.

9 Appendix

Appendices to the report are presented below.

9.1 Appendix A – Calibration

9.1.1 Catalyst synthesis

The pump used for the water flow was calibrated by weighting the pumped water after a time interval. By repeating this, a calibration curve was found for displayed water flow on pump (liquid state) against normal water flow (gas state).

Three mass flow regulators (Brooks MFC 5850E) were calibrated, one for nitrogen and two for hydrogen. The mass flow regulator used for hydrogen depended on what hydrogen flow that was used.

9.1.2 Activity and stability measurements

The mass flow controllers were calibrated by verification of already existing calibration curves. Flows used for verification were approximately equal to the flows that were to be applied in the activity measurements. The gas chromatograph was calibrated by analysing gas mixtures with known components and quantities.

9.2 Appendix B - Vaporisation experiments

Experiments to find out what temperatures of gas preheater and vaporiser that were required for a consistent vaporisation of water were performed. 8000Nml/min nitrogen and water were flowing through the system at different preheater and vaporiser temperatures. The temperature of the oven was maintained at 150°C and heating of the oven outlet was implemented since condensation of water was undesired. Temperatures of preheater and vaporiser that were investigated can be seen below in Table 9.1. The water content of the gas was set to 22vol%.

Table 9.1. Set temperatures of preheater and vaporiser in each experiment.

Name experiment	Temperature Preheater (°C)	Temperature Vaporiser (°C)
Vap104	230	155
Vap105	235	168
Vap106	240	175
Vap107		
Vap108	270	200
Vap109	296	216

As can be seen in Figure 9.1, experiments Vap04-Vap06 showed an irregular vaporisation of water; concentration peaks in the diagram suggest that the water were vaporised in turns. However, Vap107-Vap109 shows a more consistent vaporisation and hence the temperatures that were chosen for preheater and vaporiser of upcoming experiments were temperatures approximate to Vap109.

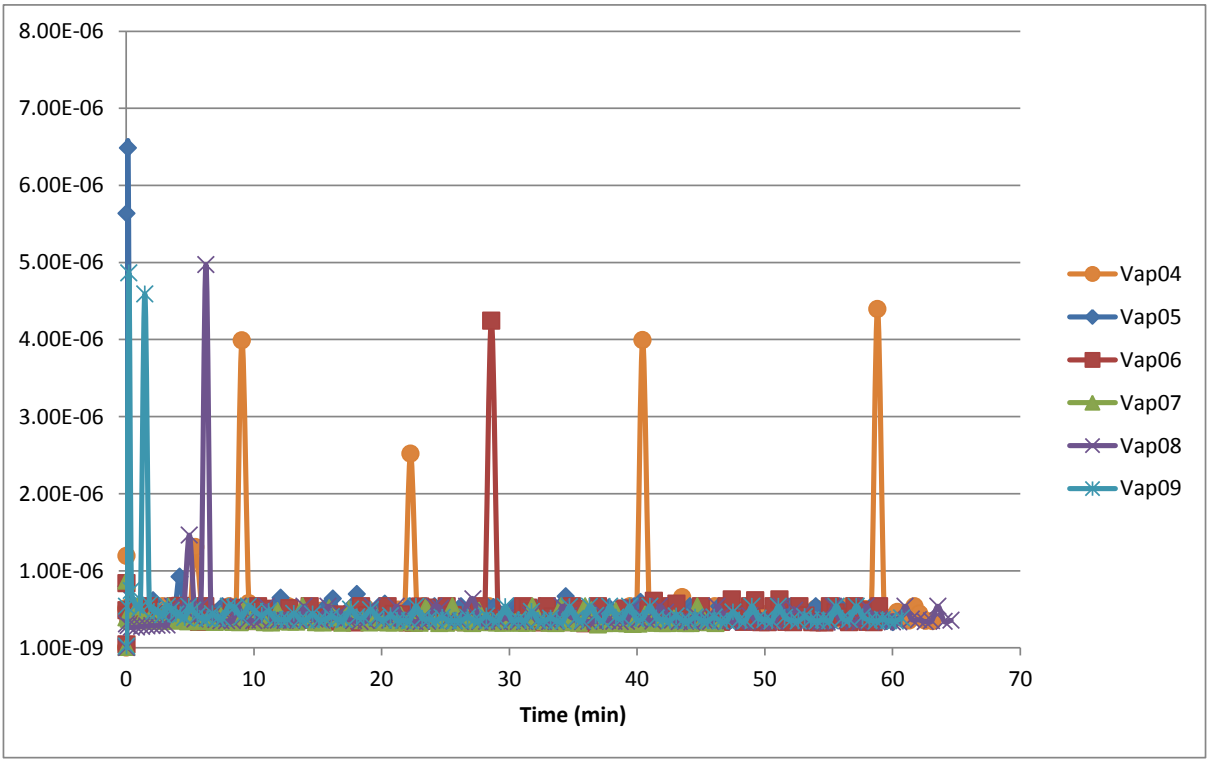

Figure 9.1. Mass spectrometer scan of water at different temperatures in preheater and vaporiser.

9.3 Appendix C –Reduction parameters

The reduction temperatures and H_2/H_2O ratios were chosen from Figure 9.4. Table 9.2, 9.3, Figure 9.2 and 9.3 shows how the reduction temperatures and H_2/H_2O ratios were approximated.

Table 9.2. Horisontal positions corresponding to Figure 9.2.

1/T * 10^3 (1/K)	**T (K)**	**T2 (°C)**	**Horizontal pos. (cm)**
1	1000	727	5.35
2	500	227	7.95
3	333.33	60.33	10.47
4	250	-23	13.01
5	200	-73	15.42

Table 9.3. Vertical positions corresponding to Figure 9.3.

ln(pH_2O/pH_2)	**pH_2O/pH_2**	**Vertical pos. (cm)**
10	2.2E+04	4.65
0	1.0E+00	8.85
-10	4.5E-05	12.95
-20	2.1E-09	17.13
-30	9.4E-14	21.3

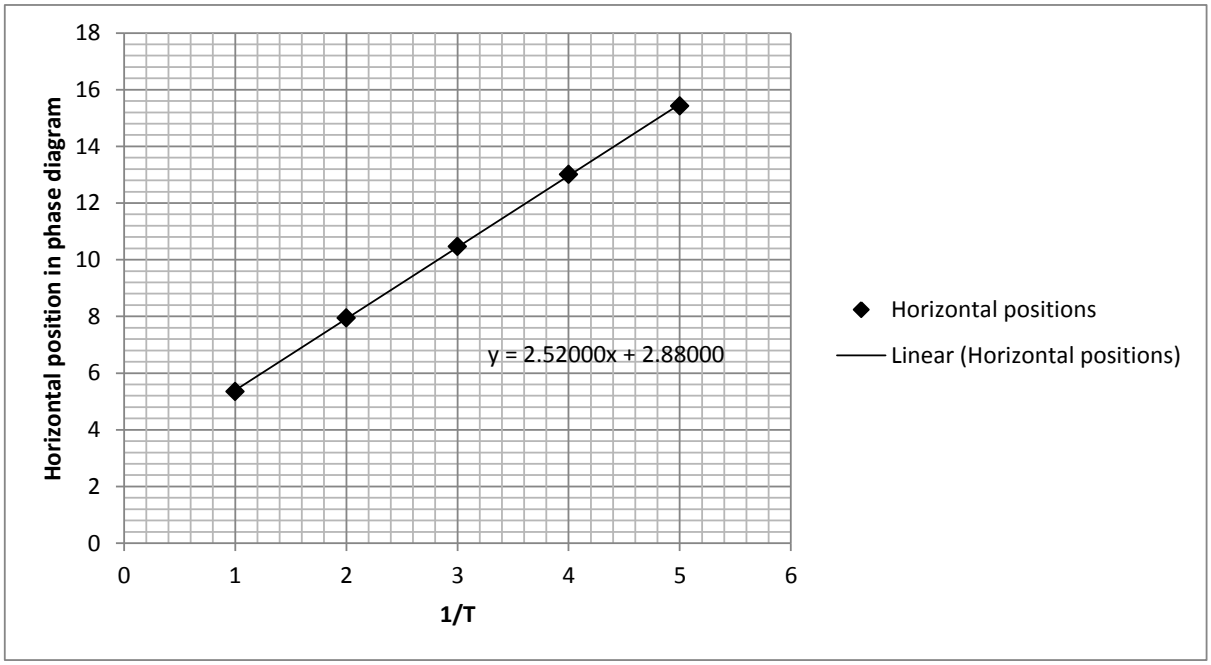

Figure 9.2. Linear dependency of horizontal positon to 1/T.

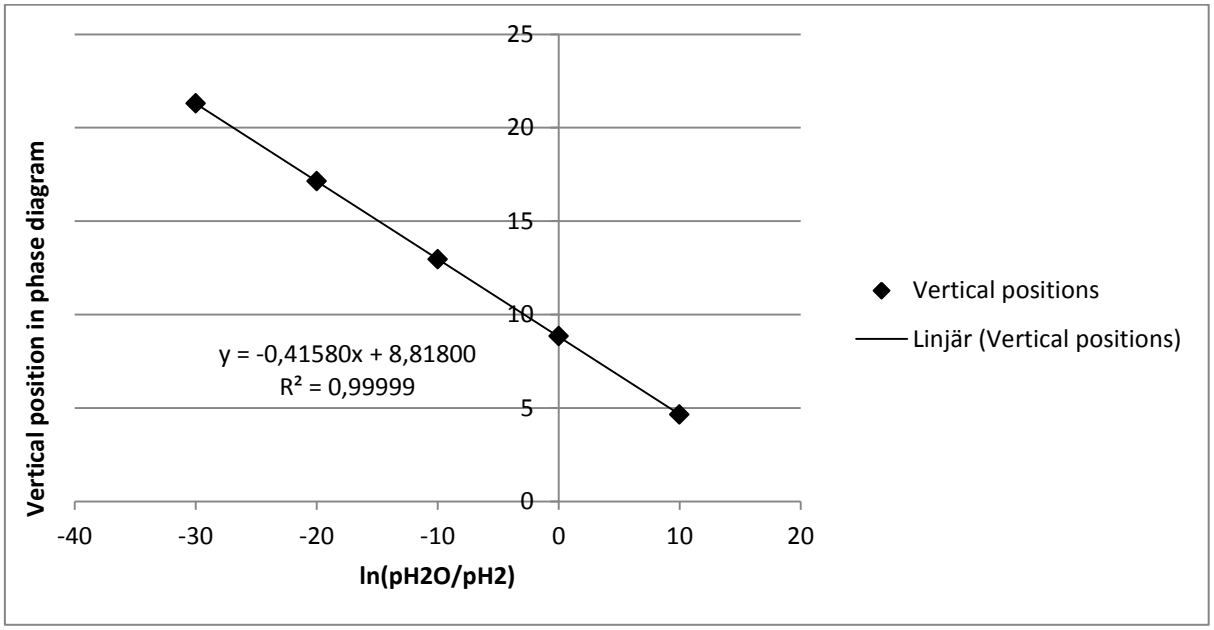

Figure 9.3. Linear dependency of vertical positions to ln(pH_2O/pH_2) were p represent partial pressure.

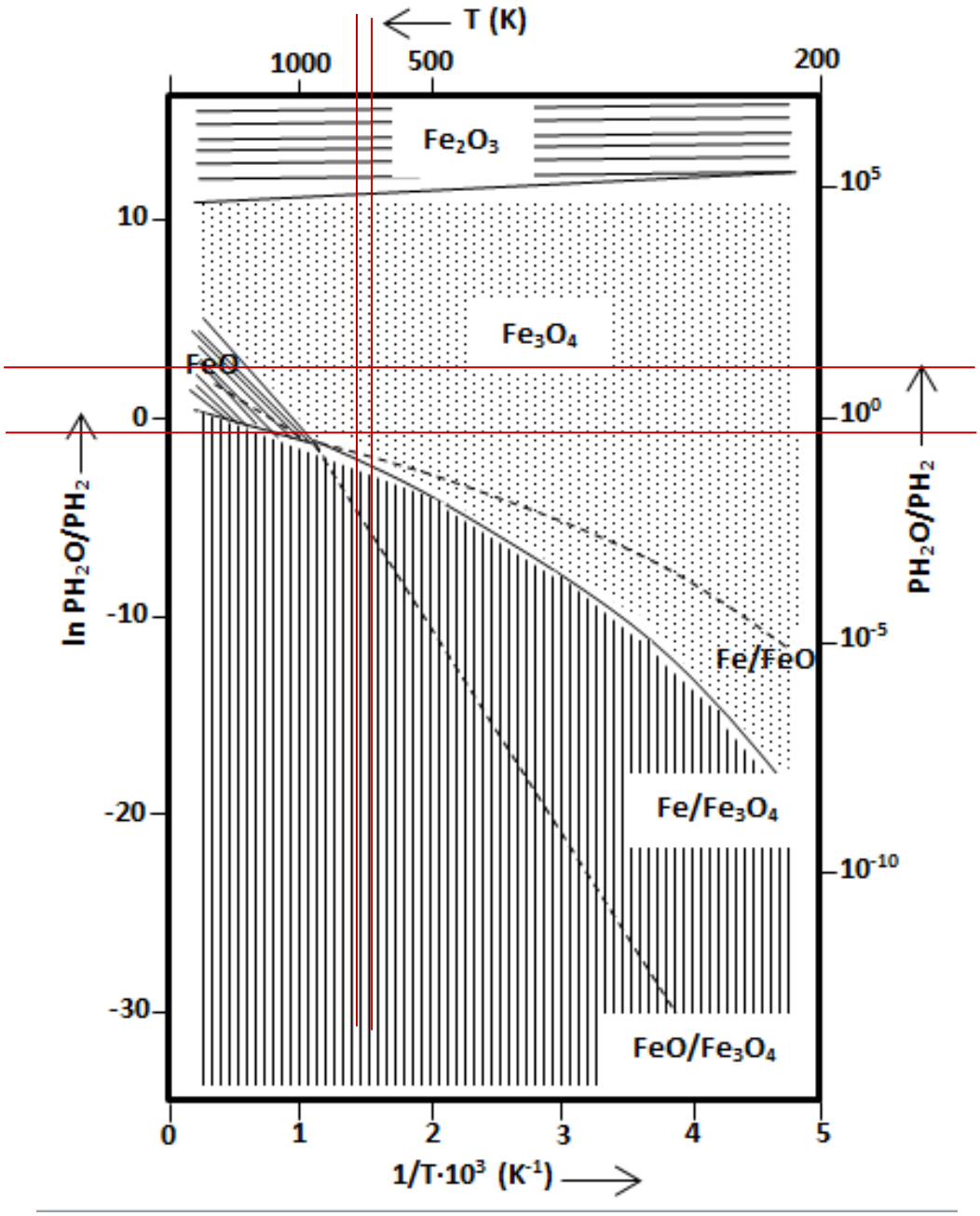

Figure 9.4. Phases diagram for iron and iron oxides where the red lines indicate at which temperature and H_2O/H_2 ratios that were targeted.

9.4 Appendix D – Additional activity data

Figure 9.5 shows concentration profiles over time when activity test was performed on R01-SD-C1 at a higher conversion than what is presented in the results. The figure corresponds to the experiment details in Table 9.4.

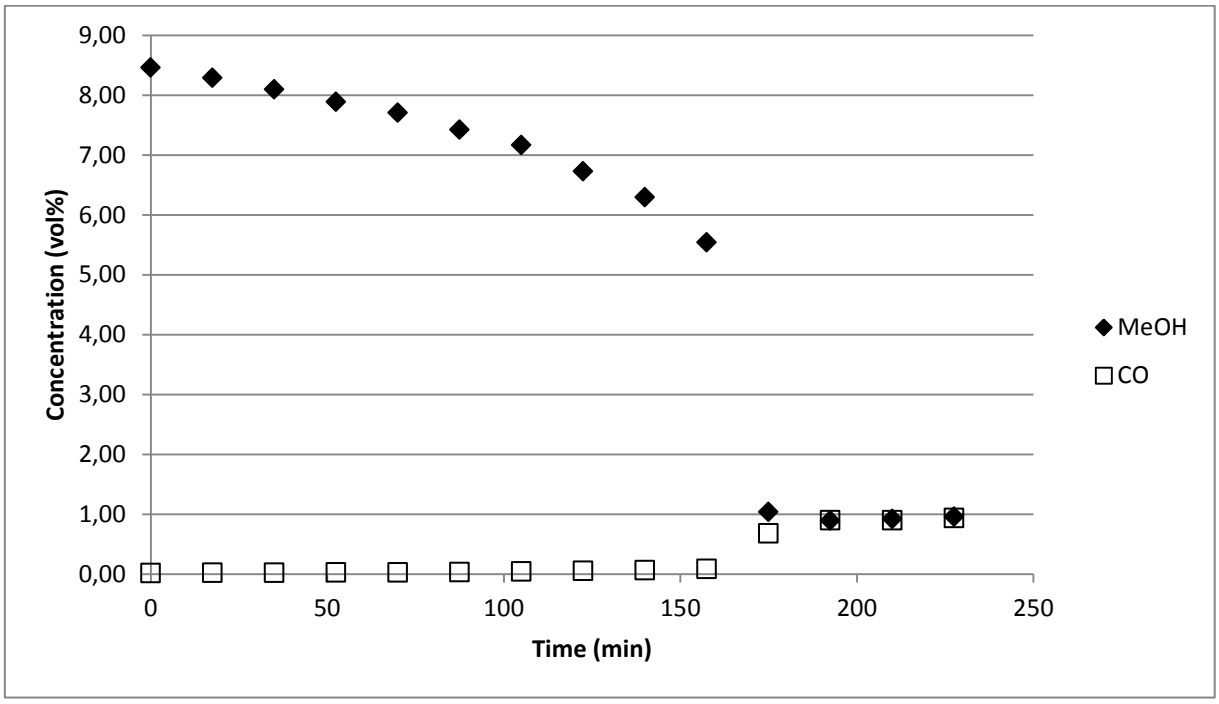

Figure 9.5. Concentration profiles of methanol and CO over time for catalyst R01-SD-C1.

Table 9.4. Details from the activity test of spinel R01-SD-C1.

Detail		Unit
Catalyst	R01-SD-C1	-
Preheater temperature	200	°C
After preheater temperature	60	°C
Tracer temperature	150	°C
Reactor block temperature (T1)	300	°C
Mass catalyst	0.2096	g
BET-surface area	23.52	m^2/g
Measured pressure reactor	0.02	barg
Theoretical gas flow	400	Nml/min
O_2 content feed	0.1	-
N_2 content feed	0.77	-
H_2O content feed	0.03	-
MeOH content feed	0.1	-

9.5 Appendix E – Stability data spinel

In this appendix data from the stability test of R01-SD-C2 is presented, see Table 9.5 and 9.6.

Table 9.5. Details from the stability test of spinel R01-SD-C2.

Detail		Unit
Catalyst	R01-SD-C2	-
Start date	29-apr	-
End date	05-maj	-
Preheater temperature	200	°C
After preheater temperature	60	°C
Tracer temperature	150	°C
Reactor block temperature (T1)	300	°C
Mass catalyst	0.2529	g
BET-surface area	19.28	m^2/g
Measured pressure reactor	0.01	barg
Theoretical gas flow	400	Nml/min
O_2 content feed	0.1	-
N_2 content feed	0.77	-
H_2O content feed	0.03	-
MeOH content feed	0.1	-

Table 9.6. Stability data.

Time	**17:34:37**	**20:52:37**	**00:10:38**	**04:01:39**
Time elapsed (h)	3.3006	6.6006	9.9008	13.9283
MeOH Conversion (%)	38.2329	33.9186	34.2091	36.1999
Methanol conversion rate (µmol/m^2/s)	2.5113	2.2279	2.2470	2.3778
FA Selectivity	78.3231	81.0178	81.7715	81.9118
CO Selectivity	1.3374	1.2045	1.1945	1.4122
CO_2 Selectivity	0.0114	0.0118	0.0119	0.0119
DME Selectivity	8.0243	10.2380	9.5563	9.0381
MF Selectivity	10.6990	4.8179	4.7781	5.0839
DMM Selectivity	1.6049	2.7101	2.6877	2.5420
Selectivity FA Eq.	79.9279	83.7279	84.4592	84.4538
Time	**07:19:40**	**10:37:40**	**13:55:41**	**17:13:42**
Time elapsed (h)	17.2286	20.5286	23.8289	27.1292
MeOH Conversion (%)	63.0634	64.9950	66.4203	69.2786
Methanol conversion rate (µmol/m^2/s)	4.1423	4.2692	4.3628	4.5506
FA Selectivity	85.5498	86.1244	86.5679	87.1031
CO Selectivity	3.9375	3.3462	3.4328	3.4457
CO_2 Selectivity	0.0126	0.0127	0.0128	0.0129
DME Selectivity	5.2500	5.0990	4.6812	4.4944
MF Selectivity	4.2656	4.4616	4.3691	4.4944
DMM Selectivity	0.9844	0.9561	0.9362	0.4494

Selectivity FA Eq.	86.5342	87.0805	87.5041	87.5526	

Time	**20:31:42**	**23:49:44**	**03:07:44**	**06:25:45**
Time elapsed (h)	30.4292	33.7297	37.7297	40.3300
MeOH Conversion (%)	72.4636	70.1015	74.6120	77.2939
Methanol conversion rate (µmol/m^2/s)	4.7598	4.6046	4.9009	5.0771
FA Selectivity	86.6512	86.8070	87.8545	87.5896
CO Selectivity	4.8755	4.1466	3.9047	4.7164
CO_2 Selectivity	0.0129	0.0129	0.0130	0.0130
DME Selectivity	4.0151	4.1466	3.9047	3.7731
MF Selectivity	4.0151	4.4427	3.9047	3.5036
DMM Selectivity	0.4302	0.4443	0.4184	0.4043
Selectivity FA Eq.	87.0814	87.2513	88.2729	87.9939

Time	**09:27:15**	**12:45:16**	**16:03:17**	**19:21:17**	**22:39:18**
Time elapsed (h)	43.3550	46.6553	49.9556	53.2556	56.5558
MeOH Conversion (%)	78.6416	79.8720	81.2185	82.0462	82.9781
Methanol conversion rate (µmol/m^2/s)	5.1656	5.2464	5.3349	5.3892	5.4504
FA Selectivity	86.8712	88.1049	87.9108	88.0278	88.1569
CO Selectivity	5.5643	4.9617	5.0103	4.9617	5.1599
CO_2 Selectivity	0.0129	0.0131	0.0131	0.0131	0.0131
DME Selectivity	3.7095	3.3949	3.5972	3.5623	3.5238
MF Selectivity	3.4446	3.1337	3.0833	3.0534	2.7687
DMM Selectivity	0.3975	0.3917	0.3854	0.3817	0.3776
Selectivity FA Eq.	87.2687	88.4966	88.2962	88.4095	88.5344

Time	**01:57:19**	**05:15:20**	**08:33:21**	**11:51:21**	**15:25:52**
Time elapsed (h)	59.8561	63.1564	66.4567	69.7567	73.3319
MeOH Conversion (%)	83.2922	84.1221	84.4216	84.9451	85.6677
Methanol conversion rate (µmol/m^2/s)	5.4711	5.5256	5.5453	5.5796	5.6271
FA Selectivity	87.7006	87.6935	89.4598	88.7868	89.6067
CO Selectivity	5.6417	5.7121	4.5823	5.5385	4.7626
CO_2 Selectivity	0.0130	0.0130	0.0133	0.0132	0.0133
DME Selectivity	3.5104	3.4769	3.4677	3.4462	3.1750
MF Selectivity	2.7582	2.7319	2.4769	2.2154	2.4423
DMM Selectivity	0.3761	0.3725	0.0000	0.0000	0.0000
Selectivity FA Eq.	88.0768	88.0660	89.4598	88.7868	89.6067

9.6 Appendix F – Stability data reference

In this appendix data from the stability test of the reference catalyst is presented, see Table 9.7 and 9.8.

Table 9.7. Details from the stability test of spinel R01-SD-C2.

Detail		Unit
Catalyst	KH44L (reference)	-
Start date		-
End date		-
Reactor block temperature	300	°C
Measured pressure reactor	0.02	barg
Theoretical gas flow	600	Nml/min
O_2 content feed	10	%
N_2 content feed	77	%
H_2O content feed	3	%
MeOH content feed	10	%

Table 9.8. Stability data.

Time	**22:47:14**	**01:47:15**	**04:47:16**	**07:47:17**
Time elapsed (h)	0	3	6	9
MeOH Conversion (%)	27.638189	28.146488	27.38334	29.561807
Methanol conversion rate (µmol/m^2/s)	9.2957223	9.4666816	9.2100072	9.9427044
FA Selectivity	73.224085	60.271033	48.967972	48.726113
CO Selectivity	0.1923122	0.2060115	0.2239748	0.208021
CO_2 Selectivity	-0.006462	-0.002323	-0.002005	0.0046269
DME Selectivity	6.6032649	6.2671925	6.494212	5.8613659
MF Selectivity	0.2857737	0.2692184	0.2272609	0.2509305
DMM Selectivity	19.701026	32.988867	44.088585	44.948942
Selectivity FA Eq.	92.925111	93.2599	93.056557	93.675056

Time	**10:47:19**	**20:26:24**	**16:49:49**	**19:49:50**
Time elapsed	12	22	41	44
MeOH Conversion	43.508455	35.056484	25.993901	25.360923
Methanol conversion rate	14.633467	11.790763	8.7426887	8.5297954
FA Selectivity	69.605669	53.639759	29.781934	25.276146
CO Selectivity	0.1423019	0.1688507	0.2264469	0.2363453
CO_2 Selectivity	-0.073477	0.0198535	-0.003761	-0.001436
DME Selectivity	3.1532773	4.3903915	6.4848151	6.6293345
MF Selectivity	0.1245393	0.1690319	0.1916327	0.1887513
DMM Selectivity	27.047689	41.612113	63.318933	67.670859
Selectivity FA Eq.	96.653358	95.251872	93.100867	92.947005

Time	22:49:51	01:49:52	04:49:53	07:49:54
Time elapsed (h)	47	50	53	56
MeOH Conversion (%)	24.835638	23.24811	23.498259	22.750024
Methanol conversion rate (µmol/m^2/s)	8.3531231	7.81918	7.9033139	7.6516555
FA Selectivity	21.511671	15.463061	16.231325	13.810154
CO Selectivity	0.2326928	0.2457045	0.2404478	0.2357421
CO_2 Selectivity	-0.007003	-0.013089	-0.011312	-0.006984
DME Selectivity	6.7277856	7.111166	7.0015927	7.2561774
MF Selectivity	0.2034378	0.1944377	0.1750113	0.1752241
DMM Selectivity	71.331417	76.99872	76.362935	78.529686
Selectivity FA Eq.	92.843087	92.46178	92.59426	92.33984

Time	10:49:55	13:49:56	16:49:57	19:49:58
Time elapsed (h)	59	62	65	68
MeOH Conversion (%)	22.522176	21.666654	21.626739	20.633753
Methanol conversion rate (µmol/m^2/s)	7.5750219	7.2872789	7.2738541	6.9398771
FA Selectivity	16.187729	13.151166	16.638297	15.126236
CO Selectivity	0.3638569	0.2354668	0.2212275	0.2274052
CO_2 Selectivity	0.019332	0.0030948	0.0005171	-0.007875
DME Selectivity	7.3156814	7.5163086	7.4662882	7.8278382
MF Selectivity	0.1588806	0.1620467	0.1690119	0.144415
DMM Selectivity	75.95452	78.931917	75.504658	76.681981
Selectivity FA Eq.	92.142249	92.083083	92.142955	91.808216

Time	22:49:59	01:50:00	04:50:01	07:50:03
Time elapsed (h)	71	74	77	80
MeOH Conversion (%)	20.169402	19.203303	17.930435	16.478378
Methanol conversion rate (µmol/m^2/s)	6.7836991	6.4587652	6.0306534	5.5422742
FA Selectivity	17.749099	18.25676	17.455609	16.932968
CO Selectivity	0.2217497	0.2341371	0.2460657	0.2498846
CO_2 Selectivity	-0.005989	-0.011822	-0.018926	0.0010644
DME Selectivity	7.9761441	8.3582759	8.9233263	9.5723372
MF Selectivity	0.1254332	0.1355908	0.1413184	0.1094325
DMM Selectivity	73.933563	73.027059	73.252607	73.134314
Selectivity FA Eq.	91.682662	91.283818	90.708216	90.067281

Time	10:50:04	13:50:05	16:50:06	19:50:07
Time elapsed (h)	83	86	89	92
MeOH Conversion (%)	15.909136	14.724755	14.352203	14.061649
Methanol conversion rate (µmol/m^2/s)	5.3508178	4.9524676	4.8271649	4.7294409
FA Selectivity	22.796438	21.353613	25.548588	31.191974
CO Selectivity	0.2532202	0.249351	0.2476093	0.251257
CO_2 Selectivity	0.0226929	0.0216065	0.0135058	0.009738

DME Selectivity	9.7775561	10.701652	11.016373	11.190737
MF Selectivity	0.1554205	0.0999799	0.0866437	0.0520023
DMM Selectivity	66.994672	67.573797	63.08728	57.304292
Selectivity FA Eq.	89.79111	88.92741	88.635868	88.496266

Time	**22:50:08**	**01:50:09**	**04:50:10**	**07:50:11**
Time elapsed (h)	95	98	101	104
MeOH Conversion (%)	12.344787	11.71952	10.506389	23.865603
Methanol conversion rate (µmol/m^2/s)	4.151998	3.9416984	3.5336785	8.0268651
FA Selectivity	28.793461	53.323553	46.700441	78.93704
CO Selectivity	0.2557094	0.2787253	0.2904337	0.0890394
CO_2 Selectivity	-0.011118	0.0082976	0.0150125	0.0348678
DME Selectivity	12.691285	13.367269	15.017045	5.8565917
MF Selectivity	0.0388222	0	0	0
DMM Selectivity	58.231841	33.022155	37.977068	15.082461
Selectivity FA Eq.	87.025302	86.345708	84.677509	94.019501

Time	**10:50:12**	**13:50:13**	**16:50:15**	**19:50:16**
Time elapsed (h)	107	110	113	116
MeOH Conversion (%)	9.0142711	15.26421	8.9836207	8.0168022
Methanol conversion rate (µmol/m^2/s)	3.0318253	5.1339058	3.0215165	2.6963404
FA Selectivity	43.510267	72.24243	58.358068	58.776718
CO Selectivity	0.3044598	0.1589334	0.2184178	0.2885206
CO_2 Selectivity	0.0809759	0.0273304	0.0180257	-0.009696
DME Selectivity	17.15962	10.080165	16.920612	19.022045
MF Selectivity	0.0256408	0	0	0
DMM Selectivity	38.919036	17.491141	24.484877	21.922413
Selectivity FA Eq.	82.429304	89.733571	82.842945	80.699131

Time	**22:50:17**	**01:50:18**	**04:50:19**	**07:50:20**
Time elapsed (h)	119	122	125	128
MeOH Conversion (%)	8.2004096	7.500842	7.2629101	6.6330297
Methanol conversion rate (µmol/m^2/s)	2.7580942	2.5228044	2.4427793	2.2309277
FA Selectivity	63.103196	58.046749	61.025314	54.188021
CO Selectivity	0.2355329	0.3017541	0.2095843	0.1579078
CO_2 Selectivity	-0.003907	-0.008765	0.0006321	0.0161453
DME Selectivity	18.537957	20.170812	20.706222	22.669685
MF Selectivity	0	0	0	0
DMM Selectivity	18.127222	21.48945	18.058248	22.968241
Selectivity FA Eq.	81.230417	79.536199	79.083562	77.156262

Time	**10:50:21**	**13:50:22**	**16:50:23**	**19:50:24**	**22:50:25**
Time elapsed (h)	131	134	137	140	143
MeOH Conversion (%)	6.9597212	5.866345	5.7405652	0.773951	5.4093067

Methanol conversion rate (µmol/m^2/s)	2.3408059	1.9730639	1.9307596	0.2603077	1.8193454
FA Selectivity	62.980072	60.198031	63.818835	-206.4443	61.102246
CO Selectivity	0.2078593	0	0.1089052	1.3770721	0
CO_2 Selectivity	0.0189062	-0.015315	0.0465407	1.5971351	0.0796736
DME Selectivity	21.305569	25.280847	25.748779	200.28449	26.803519
MF Selectivity	0.036941	0.0442916	0.1283049	0.404155	0
DMM Selectivity	15.450652	14.492146	10.148635	102.78142	12.014561
Selectivity FA Eq.	78.430725	74.690177	73.96747	-103.6629	73.116807

9.7 Appendix G – ICP-analysis data

Complete results from the ICP-analysis is presented in Table 9.8.

Table 9.9. Results from the ICP-analysis.

Test	**Fe (mg/L)**	**Mo (mg/L)**	**Theo. molar ratio**	**Mea. molar ratio**
1A (fresh, R01-SD-C1)	1316	242	0,1111	0,1069
1B (act. test, R01-SD-C1)	2262	478	0,1111	0,1231
2A (fresh, R01-SD-C2)	1169	525	0,25	0,2613
2B (stability test, R01-SD-C2)	2271	1040	0,25	0,2664